XIV

Weak interactions of heavy quarks

Heavy quarks provide a valuable guide to the study of weak interactions. Measurements of decay lifetimes and of semileptonic decay spectra of heavy, flavored mesons[1] yield information on individual elements of the CKM matrix, as does the observation of heavy-meson particle–antiparticle transitions such as B_d–$\bar{B}_d$ mixing. Long anticipated data involving detection of *CP*-violating signals have been found to be in accord with expectations of the Standard Model and have played a crucial role in constraining the sole complex phase in the CKM matrix.

XIV–1 Heavy-quark mass

At the level of the Standard Model lagrangian, the six quark masses are equivalent; they are all just input parameters that must each be determined experimentally. In the real world of particle phenomenology, quark mass divides into two sectors, 'light' (u, d, s) and 'heavy' (c, b, t). It is a hallmark of light-quark spectroscopy that hadron mass is not a direct reflection of quark mass. However, for hadrons which contain a heavy quark, the energy scale is set by the mass of the heavy quark. In the following, we discuss topics of special relevance to heavy-quark mass.

Running quark mass

Heretofore we have described the renormalization of quark mass in terms of the mass shift $\delta m = m - m_0$, where m_0 is the bare mass. We can also, for convenience, employ a multiplicative mass renormalization constant Z_m with $m_0 = Z_m m$. In minimal subtraction, Z_m will have an ϵ-expansion,

[1] Note that in the conventions of the Particle Data Group the quantum numbers of the neutral mesons are $K^0 = (d\bar{s})$, $D^0 = (c\bar{u})$, $B^0 = (d\bar{b})$ and $B_s^0 = (s\bar{b})$.

https://doi.org/10.1017/9781009291033.015 Published online by Cambridge University Press

$$Z_m\left(\alpha_s, \epsilon^{-1}\right) = 1 + \sum_{n=1}^{\infty} \frac{Z_{m,n}(\alpha_s)}{\epsilon^n} = 1 - 3C_2(\mathbf{3})\frac{\alpha_s}{4\pi}\frac{1}{\epsilon} + \cdots . \tag{1.1}$$

Both $m = m(\mu)$ and $Z_m(\mu)$ will depend implicitly on a scale μ, but not the bare mass m_0. A sequence of steps follows from this simple observation,

$$\begin{aligned} m_0 = Z_m m \qquad \text{with} \qquad \frac{dm_0}{d\ln\mu} = 0, \\ \frac{dm}{d\ln\mu} = -\frac{m(\mu)}{Z_m}\frac{dZ_m}{d\ln\mu} \equiv -\gamma_m(g(\mu))m(\mu), \\ \gamma_m = \frac{1}{Z_m}\frac{dZ_m}{d\ln\mu} = \gamma_m^{(0)}\frac{\alpha_s}{4\pi} + \gamma_m^{(1)}\left(\frac{\alpha_s}{4\pi}\right)^2 + \cdots , \end{aligned} \tag{1.2}$$

where γ_m is called the *anomalous dimension* of the quark mass operator. Since there is no explicit dependence in Z_m on either quark mass m or a renormalization scale μ, the anomalous dimension γ_m is the same in any minimally subtracted regularization scheme, such as $\overline{\text{MS}}$.

Let us determine the leading coefficient $\gamma_m^{(0)}$. From Eq. (1.2) we have[2]

$$Z_m\gamma_m(g) = \frac{dZ_m}{d\ln\mu} = 2g\frac{dg}{d\ln\mu}\frac{dZ_m}{dg^2}. \tag{1.3}$$

To proceed, we shall require an extension to $\epsilon \neq 0$ of Eq. (II–2.57b),

$$\frac{dg}{d\ln\mu} \equiv \beta(g(\mu), \epsilon) = -\epsilon g - \beta_0\frac{g^3}{16\pi^2} + \cdots = -\epsilon g + \cdots , \tag{1.4}$$

where we recall that $\beta_0 = 11 - 2n_f/3 > 0$. We then obtain from Eq. (1.3),

$$(1 + \cdots)\left(\gamma_m^{(0)} + \cdots\right) = 2g\left(-\epsilon g + \cdots\right)\left(\frac{dZ_{m,1}}{dg^2}\frac{1}{\epsilon} + \cdots\right) \tag{1.5}$$

or, finally, the desired result

$$\gamma_m^{(0)} = 6C_2(\mathbf{3}) = 8. \tag{1.6}$$

At this point, we have a differential equation whose integration gives the scale dependence of the quark mass,

$$\begin{aligned} \frac{dm(\mu)}{m(\mu)} = -\gamma_m(g(\mu))d\ln\mu, \\ d\ln\mu = \frac{d\ln\mu}{dg}dg = \frac{dg}{\beta(g)}, \\ m(\mu) = m(\mu_0)\exp\left[-\int_{g(\mu_0)}^{g(\mu)} dg'\,\frac{\gamma_m(g')}{\beta(g')}\right], \end{aligned} \tag{1.7}$$

[2] For notational simplicity, we suppress the subscript in g_3 and use instead g.

https://doi.org/10.1017/9781009291033.015 Published online by Cambridge University Press

where $\beta(g)$ is the beta function of Eq. (II–2.57b). This equation is ordinarily used for situations for which *QCD* perturbation theory is applicable (i.e. short distances). Here, we consider the leading-order expressions, with

$$\beta = -\beta_0 \frac{\alpha_s}{4\pi} g, \qquad \gamma_m = \gamma_m^{(0)} \frac{\alpha_s}{4\pi}, \tag{1.8}$$

the insertion of which into Eq. (1.7) yields

$$m(\mu) = m(\mu_0) \left[\frac{\alpha_s(\mu)}{\alpha_s(\mu_0)} \right]^{\gamma_m^{(0)}/2\beta_0}. \tag{1.9}$$

We hasten to note that the concept of a running quark mass is valid for all six flavors, not just heavy quarks. For heavy quarks, it has become standard to express the $\overline{\text{MS}}$ mass in the form $\overline{m}(\overline{m})$, i.e., to refer to the scale $\mu = \overline{m}$ which equals the $\overline{\text{MS}}$ mass itself. This is convenient because any experimental determination $\overline{m}(\mu_{\text{expt}})$ can always be 'run' to the scale $\mu = \overline{m}$. A compilation of various phenomenological inputs yields [RPP 12]

$$\overline{m}_c(\overline{m}_c) = 1.275 \pm 0.025 \text{ GeV}, \qquad \overline{m}_b(\overline{m}_b) = 4.18 \pm 0.03 \text{ GeV}. \tag{1.10}$$

Equation (1.9) represents the leading-order expression for the running mass. Extensive work on higher-order corrections has been carried out, to the level of four loops [Ch 97, VeLR 97]. An accessible recipe for a running mass at four loops is given by

$$m(\mu) = m(\mu_0) \cdot \frac{c(a_s(\mu))}{c(a_s(\mu_0))}, \tag{1.11}$$

where[3] $a_s(\mu) \equiv \alpha_s(\mu)/\pi$. In the above, the argument of the function $c(a_s(\mu))$ requires a running strong-coupling $\alpha_s(\mu)$ also evaluated at four-loop order, but this has been addressed earlier in Eqs. (II–2.77), (II–2.78). Useful numerical forms of $c(x)$ are given in [Ch 97] for each of the s, c, b, and t quarks. For example, we shall refer in Chap. XV to the b-quark version,

$$c_b(x) = x^{12/23} \left(1 + 1.17549\, x + 1.50071\, x^2 + 0.172478\, x^3\right). \tag{1.12}$$

This can be applied to run the b-quark mass from the scale $\mu_0 = \overline{m}_b(\overline{m}_b)$ to $\mu = M_H$, where M_H is the mass of the Higgs boson. We find $\overline{m}_b(M_H) \simeq 0.665\, \overline{m}_b(\overline{m}_b)$.

The pole mass of a quark

Since quarks do not exist as free particles, it should perhaps not be surprising that different theoretical definitions of quark mass appear in the literature. In the above,

[3] Note this is *not* the same as the quantity a_s appearing in Eq. (II–2.76).

https://doi.org/10.1017/9781009291033.015 Published online by Cambridge University Press

we have discussed quark mass as it is defined in the $\overline{\text{MS}}$ renormalization scheme. Another definition, the *pole mass*, is simply the renormalized quark mass in on-shell renormalization. As an example where use of pole mass seems natural, consider the top quark. Top-quark mass is measured 'directly' in collider experiments, primarily via the production of $t\bar{t}$ pairs. The t quarks will each decay as $t \to W^+b$, which ultimately gives rise to lepton + jet, dilepton, and all-jet final states. The top mass obtained by fitting invariant mass distributions of final-state particles has been interpreted as a pole mass, with recent Tevatron and LHC evaluations [Mu 12]

$$M_t = \begin{cases} 173.18 \pm 0.94 \text{ GeV} & \text{[Tevatron]} \\ 173.3 \pm 1.4 \text{ GeV} & \text{[LHC].} \end{cases} \tag{1.13}$$

There is also an 'indirect' way of determining top mass by performing a global fit of Standard Model observables in which the top quark contributes as a virtual particle.

An interesting theoretical issue is the relation between pole mass and $\overline{\text{MS}}$ mass. This has been carried out in *QCD* perturbation theory as far as three-loop order [MeR 00]. In the following we shall review this process to leading order in α_s. We begin with the inverse renormalized quark propagator, expressed as

$$S^{-1}_{F,\text{ren}}(p) = \not{p} B_{\text{ren}}(p^2, \overline{m}^2) - \overline{m} A_{\text{ren}}(p^2, \overline{m}^2), \tag{1.14}$$

where the functions A_{ren} and B_{ren} are calculated in *QCD* perturbation theory, with $\overline{m}$ being the $\overline{\text{MS}}$ mass. We must seek a zero in $S^{-1}_{F,\text{ren}}(p)$ for the on-shell conditions of $\not{p} = M$ and $p^2 = M^2$ with M being the pole mass. Following [FlJTV 99], we have for the $\mathcal{O}(\alpha_s)$ renormalized propagator amplitudes in the on-shell limit,

$$\begin{aligned} A_{\text{o-s}} \equiv A_{\text{ren}}\Big|_{\not{p}=M,\ p^2=M^2} &= 1 + \frac{\alpha_s}{4\pi} 2C_2(\mathbf{3})\,(2+\xi) + \cdots \\ B_{\text{o-s}} \equiv B_{\text{ren}}\Big|_{\not{p}=M,\ p^2=M^2} &= 1 + \frac{\alpha_s}{4\pi} 2C_2(\mathbf{3})\xi + \cdots , \end{aligned} \tag{1.15}$$

where ξ is the gauge parameter and $C_2(\mathbf{3})$ is given below Eq. (II–2.12). We can now obtain the desired relation between pole mass M and $\overline{\text{MS}}$ mass $\overline{m}$ in terms of the $\overline{\text{MS}}$ coupling $\hat{\alpha}_s$. The condition for a zero, $0 = mA_{\text{o-s}} - MB_{\text{o-s}}$, implies the relation,

$$M = \overline{m}\frac{A_{\text{o-s}}}{B_{\text{o-s}}} = \overline{m}(M)\left[1 + C_2(\mathbf{3})\frac{\hat{\alpha}_s(M)}{\pi} + \cdots\right], \tag{1.16}$$

where we exhibit scale dependence in $\overline{m}$ or α_s as it would appear in a more general treatment. Notice that the explicit gauge dependence has canceled, as it must.

For the top quark, a comparison between $\overline{\rm MS}$ mass and pole mass at NNLO level in the *QCD* perturbation theory gives

$$\overline{m}_t(\overline{m}_t) = 163.3 \pm 2.7 \text{ GeV}, \qquad M_t = 173.3 \pm 2.8 \text{ GeV}, \tag{1.17}$$

as inferred from Tevatron data [AlDM 12].

Actually, it would appear that the very concept of pole mass for a quark is paradoxical because, after all, quarks are *not* free particles, and it is, in fact, the case that due to confinement the exact nonperturbative quark propagator will not have a pole. The pole mass exists as a creature of perturbation theory and phenomenology. There is, however, a price to pay for this convenience. Calculation has shown that there will be higher orders which grow factorially in the perturbation expansion [BeB 95, BiSUV 94]. Because of this, the pole mass itself cannot be determined to an accuracy better than the confinement scale Λ_{QCD}. Other definitions of the mass parameter include the $1S$ *mass*, defined as one-half the energy of the $1S\ Q\bar{Q}$ state [HoLM 99], and the *kinetic mass*, defined via a threshold in weak decay [BiSUV 94]. Because these include the effects of confinement, they turn out to be better behaved in many perturbative calculations [ElL 02]. Indeed, even for the top quark the $1S$ mass is prefered for a proper theoretical description of the $t\bar{t}$ production cross section near threshold [HoT 99].

Our lack of understanding of the large magnitude of the top mass illustrates how little we actually know about the mechanism of mass generation. If all fermion masses arise from the Yukawa interaction of a single Higgs doublet, then the Yukawa coupling constants must vary by the factor $g_t/g_e = m_t/m_e \sim 3 \times 10^5$. There is nothing inconsistent about such a variation, but it is so striking as to beg for a logical explanation, one which is presently lacking.

XIV–2 Inclusive decays

Heavy quarks decay to a large number of final states, often containing many particles. As the mass of the heavy quark gets larger, it makes increasing sense to treat the final states inclusively. We discuss this approach in this section.

The spectator model

Consider the weak beta decay, $Q \to q\bar{e}\nu_e$, of an isolated heavy quark Q into a lighter quark q. By analogy with muon decay, this proceeds with decay rate (if radiative corrections are ignored)

$$\Gamma_{Q\to q\bar{e}\nu_e} = \frac{G_F^2 m_Q^5}{192\pi^3} \left|V_{qQ}\right|^2 f(m_q/m_Q),$$
$$f(x) = 1 - 8x^2 + 8x^6 - x^8 - 24x^4 \ln x \tag{2.1}$$

https://doi.org/10.1017/9781009291033.015 Published online by Cambridge University Press

where $f(x)$ is the phase-space factor already encountered in our discussion of muon decay in Sect. V–2 and of tau decay in Sect. V–3. Under what circumstances would this be a good representation for the beta decay of a heavy-*meson*-containing quark Q? For it to be accurate, the final state must develop independently of the other (so-called *spectator*) quark in the heavy meson. Experience with deep-inelastic scattering suggests that this occurs when the recoiling quark q carries energy and momentum larger than typical hadronic scales, i.e., in the range $E_q > 1$–1.5 GeV. For D decays, the average light-quark energy is $\langle E_q \rangle \sim m_D/3 \simeq 0.5$ GeV, in which case this approximation is suspect. It should be considerably better in B decays, but still not perfect.

Let us explore the consequences of adopting the spectator model for D and B decays. If we neglect CKM-suppressed modes, the main decay channels for b quarks are $b \to c\bar{u}d, c\bar{c}s, c\ell\bar{\nu}_\ell$ ($\ell = e, \mu, \tau$), while for c quarks they are restricted to $c \to s\bar{d}u, s\bar{\mu}\nu_\mu, s\bar{e}\nu_e$. Relative to the lepton modes, each hadronic decay channel picks up an additional factor of 3 upon summing over the final-state colors. Two of the B-meson final states ($c\bar{c}s$ and $c\tau\bar{\nu}_\tau$) have significant phase-space suppressions (reducing them to about 20% of the $c\bar{u}d$ mode) due to the heavy masses involved. The simplest spectator model then predicts branching ratios

$$\begin{aligned} \mathrm{Br}_{D\to\bar{e}\nu_e X} &\simeq \frac{1}{3+2} = 0.2, \\ \mathrm{Br}_{B\to e\bar{\nu}_e X} &\simeq \frac{1}{3\times(1+0.2)+2+0.2} = 0.17 \end{aligned} \tag{2.2}$$

where X denotes a sum over the remaining final-state particles. Also, this picture predicts the absolute rates of the D and B decays to be

$$\tau_D = \left[5\frac{G_F^2 m_c^5}{192\pi}\,|V_{\rm cs}|^2\, f(x_c)\right]^{-1} \simeq 1.1\times 10^{-12}\,\mathrm{s}, \tag{2.3a}$$

$$\tau_B = \left[5.8\frac{G_F^2 m_b^5}{192\pi^2}\,|V_{\rm cb}|^2\, f(x_b)\right]^{-1} \simeq 1.8\times 10^{-12}\,\mathrm{s}\left|\frac{0.041}{V_{\rm cb}}\right|^2, \tag{2.3b}$$

where $f(x_c) \simeq 0.7$ and $f(x_b) \simeq 0.5$ are phase-space factors. For definiteness, we have taken $m_c = 1.5$ MeV and $m_b = 4.9$ GeV in the above. However, note the quintic dependence on quark mass; the B-lifetime prediction would be 10% lower if $m_b = 5.0$ GeV were used!

For D decays, the D^+ and D^0 lifetimes differ by a factor of about 2.5,

$$\tau_{D^+} = (10.40 \pm 0.07)\times 10^{-13}\,\mathrm{s}, \qquad \tau_{D^+}/\tau_{D^0} = 2.54 \pm 0.02, \tag{2.4}$$

whereas the spectator model requires them to be equal. This failure is not surprising, as the D-meson mass lies in the region of strong hadronic resonances; final-state interactions can seriously disturb the spectator picture. Thus, we expect the spectator model to reveal only gross features of the D system. It is remarkable, given its simplicity, that the spectator model predicts (roughly) the correct magnitudes of the lifetime and of the inclusive branching ratios,

$$\mathrm{Br}_{D^0\to e\bar{\nu}_e X} = (6.49 \pm 0.11)\%, \qquad \mathrm{Br}_{D^+\to e\bar{\nu}_e X} = (16.07 \pm 0.30)\%. \tag{2.5}$$

We see that the decays of the D^+ correspond more closely to the spectator predictions than do those of the D^0. The D^0-hadronic decay modes are notably greater that the expectation of the spectator model.

Even for B mesons, the spectator model provides only a rough guide. The lifetimes of the different-flavored B mesons are reasonably similar

$$\begin{aligned} \tau_{B^0} &= (1.519 \pm 0.0.007) \times 10^{-12}\,\mathrm{s}, \\ \frac{\tau_{B^+}}{\tau_{B^0}} &= 1.079 \pm 0.007, \\ \frac{\tau_{B_s^0}}{\tau_{B^0}} &= 0.986 \pm 0.011, \end{aligned} \tag{2.6}$$

and the spectator estimate differs from these by less than 20%. However, the spectator prediction for the leptonic branching ratio is about 60% larger than the experimental value

$$\mathrm{Br}_{B\to e\bar{\nu}_e X} = (10.72 \pm 0.13)\,\%, \tag{2.7}$$

where the number quoted corresponds to roughly an equal mixture of B^+ and B^0. The shorter lifetime and lower leptonic branching ratio point to a modest enhancement of the hadronic modes.

The heavy-quark expansion

The spectator model can be transformed into a solid *QCD* calculation through the use of the operator-product expansion (OPE) [ChGG 90, Ne 05]. This allows the inclusion of perturbative and nonperturbative corrections.

Using the B meson as our example, the treatment starts by considering the current matrix element, squared and summed over all final states,

$$W_{\alpha\beta} = (2\pi)^4 \sum_X \delta^4(P_B - q - P_X)\langle B(v)|J_\alpha^\dagger|X\rangle\langle X|J_\beta|B(v)\rangle, \tag{2.8}$$

where q is the momentum carried by the current. The total decay rate is obtained by combining $W_{\alpha\beta}$ with the squared lepton current matrix element $L^{\alpha\beta}$,

$$L^{\alpha\beta} = 4\left(p_\ell^\alpha p_\nu^\beta + p_\ell^\beta p_\nu^\alpha - g^{\alpha\beta} p_\ell \cdot p_\nu + i\epsilon^{\alpha\beta\gamma\delta} p_{\ell\gamma} p_{\nu\delta}\right), \tag{2.9}$$

and integrating over phase space.

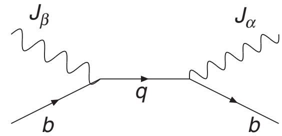

Fig. XIV–1 The leading contribution to the heavy-quark expansion.

The on-shell tensor $W_{\alpha\beta}$ is given by the discontinuity in the full tensor

$$T_{\alpha\beta} = -i \int d^4x \, e^{-iq\cdot x} \langle B(v)|T(J_\alpha^\dagger(x)J_\beta(0))|B(v)\rangle, \tag{2.10}$$

related by $W_{\alpha\beta} = -\pi \operatorname{Im} T_{\alpha\beta}$. The discontinuity is evaluated at the physical cut, which extends over the region

$$m_B\sqrt{q^2} \le m_B v\cdot q \le \frac{1}{2}(m_B^2 + q^2 - m_j^2), \tag{2.11}$$

where m^j is the lightest hadron for the final-state quark q_j, i.e., m_π for $q_j = u$ or m_D for $q^j = c$. In this formalism, the spectator calculation arises from the evaluation of the diagram in Fig. XIV–1 using the free intermediate-state propagator. For a current $\bar{q}\Gamma_\alpha b = \bar{q}\gamma_\alpha(1+\gamma_5)b$, the tensor $T_{\alpha\beta}$ becomes

$$\begin{aligned} T_{\alpha\beta} &= -i \int d^4x \, e^{-iq\cdot x} \langle B(v)|\bar{b(x)}\Gamma_\alpha S_F(x)\Gamma_\beta b(0)|B(v)\rangle \\ &= \langle B(v)|\frac{2}{p^2 - m_q^2 + i\epsilon} \cdot \mathcal{M}_{\alpha\mu\beta} \cdot \bar{b}\gamma^\mu(1+\gamma_5)b|B(v)\rangle, \end{aligned} \tag{2.12}$$

where $\mathcal{M}_{\alpha\mu\beta} \equiv g_{\alpha\mu}p_\beta + g_{\beta\mu}p_\alpha - g_{\alpha\beta}p_\mu - i\epsilon_{\alpha\beta\mu\nu}p^\nu$ with $p^\mu = mv^\mu - q^\mu$ being the momentum carried by the intermediate propagator. The only nonzero matrix element for a B hadron at rest is $\langle B|\bar{b}\gamma^0 b|B\rangle = 1$. In this case, the amplitude is equivalent to the free decay of a b quark.

However, one can do better because the short-distance behavior of the full tensor can be described by an OPE. Because the heavy b quark carries a high energy and transfers that energy to the intermediate states, the region of validity of the OPE is somewhat different than our previous discussion for the weak hamiltonian [ChGG 90]. As $v\cdot q$ approaches the upper range given in Eq. (2.11), the overall hadronic mass becomes smaller and enters the region where binding becomes important and perturbation theory fails.

There are two key improvements that can be accomplished by this method. One is the addition of perturbative corrections. Included in this process is the ability to connect the b-quark mass to a perturbatively well-defined definition of that mass. This tames the strong m_b^5 dependence found in the spectator model by relating the b mass to a well-defined observable. In practice, mass definitions which are tied to measurements that already include confinement effects, such as the $1S$ mass or the kinetic mass mentioned in Sect. XIV–1, provide the most stable perturbative definition [BiSUV 94, HoLM 99]. The other path of improvement is to include new operators that describe nonperturbative hadronic matrix elements [BiSUV 93, Ma 94, MaW 94]. These new operators enter in an expansion in the inverse of the heavy-quark mass. The leading operators are those discussed for the heavy-quark expansion in the preceding chapter. We can see how these arise by expanding the tensor $T_{\alpha\beta}$ around the heavy-quark limit including interactions. The interactions can be seen in the full propagator

$$S_q(x) = \langle x|\frac{1}{\not{D} - m_q + i\epsilon}|0\rangle = \langle x|(\not{D} + m_q)\frac{1}{D^2 + \frac{g_3\lambda^a}{4}\sigma^{\mu\nu}F^a_{\mu\nu} - m_q + i\epsilon}|0\rangle, \tag{2.13}$$

where $\not{D}$ contains the full covariant derivative including the gauge potential and we have used Eq. (III–3.50) in obtaining the second form. When the matrix element is taken, the derivative turns into $D^\mu = (mv^\mu - q^\mu) + d^\mu$ where d^μ contains the residual momenta and the gauge field. The result is an OPE of the form

$$T(J^{\dagger\alpha}(x)J^\beta(0)) = c_1^{\alpha\beta}\bar{b}b + \frac{c_2^{\alpha\beta}}{m_b^2}\bar{b}(i\mathbf{D})^2 b + \frac{c_3^{\alpha\beta}}{m_b^2}\bar{b}\frac{it^a}{2}\sigma_{ij}F^{aij}b. \tag{2.14}$$

To leading order in $1/m_b$, the result can then be expressed in terms of the two matrix elements

$$\mu_\pi^2 = \langle B(v)|\bar{b}(i\mathbf{D})^2 b|B(v)\rangle, \qquad \mu_G^2 = \langle B(v)|\bar{b}\frac{it^a}{2}\sigma_{\mu\nu}F^{a\mu\nu}b|B(v)\rangle. \tag{2.15}$$

The overall inclusive result has the form [BeBMU 03]

$$\Gamma(B \to X_c e\nu) = \frac{G_F^2 m_b^5(\mu)}{192\pi^3}|V_{bc}|^2\left[f\left(\frac{m_q}{m_Q}\right)(1 + O(\alpha_s))\left(1 - \frac{\mu_\pi^2 - \mu_G^2}{2m_b^2}\right) - 2\left(1 - \frac{m_c^2}{m_b^2}\right)^4\frac{\mu_G^2}{m_b^2} + \cdots\right]. \tag{2.16}$$

The gluonic operator also appears in the description of the spectroscopy of heavy quarks, as described in Chap. XIII, and its value can be estimated from the mass splittings in heavy hadrons. The kinetic operator can be fit as part of the energy distribution of semileptonic B decay in a combined fit with the total decay rate. The perturbative corrections depend on which definition of the renormalized mass is employed. Further refinements include the perturbative scaling of the coefficients of μ_i and the addition of $1/m_b^3$ effects.

Inclusive measurements can be used to extract the CKM elements [RPP 12],

$$V_{\rm cb} = (41.88 \pm 0.44 \pm 0.59) \times 10^{-3}, \qquad V_{\rm ub} = (4.41 \pm 0.15 \pm 0.16) \times 10^{-3}. \tag{2.17}$$

The top quark

The top quark is the real heavyweight of the quarks and presents a rather novel decay pattern. Because $m_t > M_W + m_b$ and the CKM element $|V_{\rm tb}|$ is near unity, the dominant decay is the *semiweak* transition $t \to b + W^+$. The amplitude and transition rate for this process are

$$\begin{aligned} \mathcal{M}_{t\to bW^+} &= -i\,\frac{g_2}{\sqrt{8}} V_{\rm tb}^* \epsilon_\mu^*(\mathbf{p}_W)\overline{u}(\mathbf{p}_b)\gamma^\mu(1+\gamma_5)u(\mathbf{p}_t), \\ \Gamma_{t\to bW^+} &= \frac{G_F m_t^3}{8\pi\sqrt{2}}|V_{\rm tb}|^2\left[1 - 3\frac{M_W^2}{m_t^2} + 2\frac{M_W^4}{m_t^4}\right], \end{aligned} \tag{2.18}$$

where we have neglected the b quark mass in the decay rate. The question of which definition of m_t to use can be answered only when including *QCD* radiative corrections, and the convergence of the perturbative series is best when using a short-distance definition of the mass, such as the $\overline{\rm MS}$ mass, rather than the pole mass [BeB 95]. *QCD* corrections including gluon radiation have now been carried out to second order in α_s [CzM 99, ChHSS 99]. Including these, the top width is [BeE *et al*. 00]

$$\Gamma_t = 1.42 \text{ GeV}, \tag{2.19}$$

corresponding to a lifetime of $\tau = 4.6 \times 10^{-25}$ s. For such a large t-quark mass, the emitted W^+ bosons are predominantly longitudinally polarized, exceeding production of transversely polarized W^+ bosons by a factor $\sim m_t^2/M_W^2$. This is a reflection of the large Yukawa coupling of the t quark to the (unphysical) charged Higgs scalar, which becomes the longitudinal component of the W^+. Other decay modes of the t quark will be highly suppressed by weak mixing factors, e.g., for the mode $t \to s + W^+$ the suppression amounts to $|V_{\rm ts}/V_{\rm tb}|^2 \simeq 1.6 \times 10^{-3}$.

An interesting consequence of the large $t \to b + W^+$ quark decay rate is that there will not be sufficient time for the top quark to form bound-state hadrons. In view of the large top-quark mass, the $t\bar{t}$ system (*toponium*) is nonrelativistic and sits in an effectively Coulombic potential, $V = -4\alpha_s/3r$. In the ground state, one finds the quark velocity $v_{\rm rms} = 4\alpha_s/3$ and atomic radius $r_0 = 3/(2\alpha_s m_t)$. A characteristic orbital period is then $T = 2\pi r_0/v_{\rm rms} = 9\pi/(4\alpha_s^2 m_t)$. Using $\alpha_s(r_0) = 0.12$, we estimate $T = 19 \times 10^{-25}$ s. In contrast, the toponium lifetime would be one-half the t lifetime given above, since either t or $\bar{t}$ could decay first. These comparisons imply that the top quark has an appreciable probability of decaying before completion of even a single bound-state orbit. An equivalent indication of the same effect is the observation that the toponium weak decay width (twice that of a single top quark) is larger than the spacing between energy levels, such as $E_{2S} - E_{1S} = \alpha_s^2 m_t/3 \sim 0.9$ GeV. The production cross section does not then occur through sharp resonances. Instead, there exists a rather broad and weak threshold enhancement, due to the attractive nature of the Coulombic potential. This permits the production and decay of top quarks to be analyzed perturbatively, with Γ_t serving as the infrared cut-off. A heavy top quark can then provide a new laboratory for perturbative *QCD* studies.

XIV–3 Exclusive decays in the heavy-quark limit

The spectator model calculates the decay rates as if the final-state quarks were free. However, the actual decays take place to physical hadronic final states. For the total rate, there is absolutely no hope of reliably calculating and summing all the individual nonleptonic decays. For semileptonic decays, the situation is somewhat better. The data show that the quasi-one-hadron states, i.e., $D \to K\bar{e}\nu_e$, $K^*\bar{e}\nu_e$ and $B \to De\bar{\nu}_e$, $D^*e\bar{\nu}_e$, form the largest component of the semileptonic rates,

$$\frac{\Gamma_{D^+\to K\bar{e}\nu_e + K^*\bar{e}\nu_e}}{\Gamma_{D^+\to X\bar{e}\nu_e}} = 0.89 \pm 0.03, \qquad \frac{\Gamma_{B^+\to De\bar{\nu}_e + D^*e\bar{\nu}_e}}{\Gamma_{B^+\to X_c e\bar{\nu}_e}} = 0.74 \pm 0.05. \quad (3.1)$$

These transitions can be addressed by quark model calculations, so that we have an independent handle on such decays. The hadronic-current matrix elements are described by form factors such as

$$\begin{aligned}
\langle K^-(\mathbf{p}')\left|\bar{s}\gamma_\mu c\right| D^0(\mathbf{p})\rangle &= f_+\left(p + p'\right)_\mu + f_-\left(p - p'\right)_\mu \ , \\
\langle K^{*-}(\mathbf{p}')\left|\bar{s}\gamma_\mu c\right| D^0(\mathbf{p})\rangle &= ig\epsilon_{\mu\nu\alpha\beta}\epsilon^{*\nu}\left(p + p'\right)^\alpha \left(p - p'\right)^\beta , \\
\langle K^{*-}(\mathbf{p}')\left|\bar{s}\gamma_\mu\gamma_5 c\right| D^0(\mathbf{p})\rangle &= f_1\epsilon_\mu^* + \epsilon^*\cdot q\left[f_2\left(p + p'\right)_\mu + f_3\, q_\mu\right], \qquad (3.2)
\end{aligned}$$

with analogous definitions for the B decays. All form factors are functions of the four-momentum transfer $q^2 = (p - p')^2$. The physics underlying these form factors is two-fold:

(1) If the final-state meson does not recoil, the amplitude is determined by an overlap of the quark wavefunctions, as described in Sect. XII–2.
(2) As the final-state meson recoils, the wavefunction overlap becomes smaller, so that the form factors fall off with increasing recoil momentum.

For D decays, the CKM element is known to a high degree of accuracy from the unitarity of the CKM matrix. In this case, lattice or quark model calculations serve to check whether the experimental rate can be reproduced. For B decays involving

https://doi.org/10.1017/9781009291033.015 Published online by Cambridge University Press

the $b \to c$ transition, the exclusive rates are treated using Heavy Quark Effective Theory, which we will describe below.

In the case of *nonleptonic* B, D decays, we have considerably less confidence in our ability to predict the decay amplitudes. This is especially true in D nonleptonic decay because the rescattering corrections required by unitarity can play a major role. Unitarity predicts (cf. Eq. (C–3.14)) for the $D \to f$ matrix element of the transition operator,

$$i(\mathcal{T} - \mathcal{T}^\dagger)_{D\to f} = \sum_n \mathcal{T}^*_{n\to f}\mathcal{T}_{n\to D}, \tag{3.3}$$

where n are the physically allowed intermediate states. The scattering matrix elements are evaluated at the mass of the D, which happens to lie in an energy range where many strong resonances lie. The scattering elements $\mathcal{T}_{n\to f}$ are therefore expected to be of order unity, implying that rescattering can mask the underlying pattern of weak matrix elements. This makes calculation of nonleptonic D decays particularly suspect.

Inclusive vs. exclusive models for $b \to ce\bar{\nu}_e$

Inclusive and exclusive techniques appear conceptually quite different, even if we know that the total inclusive rate is made from a sum of exclusive individual modes. However, the following observation [ShV 88] is instructive for connecting the two methods.

Consider the semileptonic decay of a heavy quark into another heavy quark, $Q_a \to Q_b e\bar{\nu}_e$, such that their mass difference Δm is small compared to the average of their masses ($(m_a + m_b)/2 \gg \Delta m$), yet large compared to the QCD scale ($\Delta m \gg \Lambda_{QCD}$). Because of the second condition, one might use the spectator model result,

$$\Gamma_{Q_a\to Q_b e\bar{\nu}_e} \simeq \frac{G_F^2(m_a - m_b)^5}{15\pi^3}\,|V_{ab}|^2\,, \tag{3.4}$$

where V_{ab} is the appropriate weak-mixing matrix element. However, if the first condition is satisfied, the quark recoil will be nonrelativistic. This leads to a nonrelativistic calculation of the transitions from a pseudoscalar $Q_a\bar{q}$ state to pseudoscalar and to vector $Q_b\bar{q}$ states. In this limit, $\bar{\psi}_b\gamma_0\psi_a \to \psi_b^\dagger\psi_a$ is proportional to the normalization operator, while the axial current $\bar{\psi}_b\gamma_i\gamma_5\psi_a \to \psi_b^\dagger\sigma_i\psi_a$ is proportional to the spin operator. For states normalized as

$$\langle (Q_a\bar{q})^{0^-}_{\mathbf{p}'}\,\big|\,(Q_a\bar{q})^{0^-}_{\mathbf{p}}\rangle = 2m\,\delta^3(\mathbf{p} - \mathbf{p}'), \tag{3.5}$$

https://doi.org/10.1017/9781009291033.015 Published online by Cambridge University Press

one then has

$$\langle (Q_b\bar{q})^{0^-}_{\mathbf{p}'} \left| \bar{\psi}_b \gamma_0 \psi_a \right| (Q_a\bar{q})^{0^-}_{\mathbf{p}} \rangle = 2m \ ,$$
$$\langle (Q_b\bar{q})^{1^-}_{\mathbf{p}'} \left| \bar{\psi}_b \gamma_i \gamma_5 \psi_a \right| (Q_a\bar{q})^{0^-}_{\mathbf{p}} \rangle = 2m \ \epsilon_i^{\dagger}(\mathbf{p}'), \tag{3.6}$$

where m is either m_a or m_b. This translates into invariant form factors

$$\langle (Q_b\bar{q})^{0^-}_{\mathbf{p}'} \left| \bar{\psi}_b \gamma_\mu \psi_a \right| (Q_a\bar{q})^{0^-}_{\mathbf{p}} \rangle = \left(p + p'\right)_\mu ,$$
$$\langle (Q_b\bar{q})^{1^-}_{\mathbf{p}'} \left| \bar{\psi}_b \gamma_\mu \gamma_5 \psi_a \right| (Q_a\bar{q})^{0^-}_{\mathbf{p}} \rangle = 2m \ \epsilon_\mu^{\dagger}(\mathbf{p}'), \tag{3.7}$$

which are the correct relativistic results. Using these to calculate the semileptonic decays, one finds

$$\Gamma_{(Q_a\bar{q})_{0^-} \to (Q_b\bar{q})_{0^-} e\bar{\nu}_e} = \frac{G_F^2}{60\pi^3} (m_a - m_b)^5 \left|V_{ab}\right|^2 ,$$
$$\Gamma_{(Q_a\bar{q})_{0^-} \to (Q_b\bar{q})_{1^-} e\bar{\nu}_e} = \frac{G_F^2}{20\pi^3} (m_a - m_b)^5 \left|V_{ab}\right|^2 . \tag{3.8}$$

Comparing these, one sees that the sum of the pseudoscalar and vector widths exactly saturates the spectator result of Eq. (3.4). In this combined set of limits, it seems that both types of calculations can be valid simultaneously. Direct application of this insight to $b \to ce\bar{\nu}_e$ decays is somewhat marginal, as the nonrelativistic condition is not well satisfied. A velocity as large as $v = 0.8c$ is reached in portions of the decay region, although on the average a lower value is obtained. However, it is likely that the near equality of spectator versus quark model results is a remnant of the situation described above.

Heavy Quark Effective Theory and exclusive decays

The discussion of the previous section leaned heavily on the use of models to describe quark weak decay. However, many aspects of weak transitions can be obtained in a model-independent fashion through the use of the $m_Q \to \infty$ limit, which was introduced in Sect. XIII–3. This effective theory provides a variety of qualitative and quantitative insights of considerable value.

The heavy-quark approximation manages to justify many results which have become part of the standard lore of quark models. For example, consider the decay constant of a $Q\bar{q}$ pseudoscalar meson M,

$$\langle 0 \left| \bar{q}(x) \gamma^\mu \gamma_5 Q(x) \right| M(\mathbf{p}) \rangle = i\sqrt{2}\, F_M p^\mu \, e^{-ip\cdot x} . \tag{3.9}$$

In the quark model one finds that $F_M \propto (m_M)^{-1/2}$. This follows from the normalization of momentum eigenstates,

$$\langle M(\mathbf{p}') | M(\mathbf{p}) \rangle = 2E_{\mathbf{p}} \delta^{(3)}(\mathbf{p} - \mathbf{p}'), \tag{3.10}$$

https://doi.org/10.1017/9781009291033.015 Published online by Cambridge University Press

such that

$$\langle 0|\bar{q}\gamma_0\gamma_5 Q|M(0)\rangle = \begin{cases} i\sqrt{2}\,F_M m_M & \text{(decay const defn.)}, \\ i\sqrt{2m_M}\,\psi(0)\sqrt{2N_c} & \text{(quark model reln.)}, \end{cases} \tag{3.11}$$

where $\psi(0)$ is the $Q\bar{q}$ wavefunction at the origin and N_c is the number of colors. Since, as $m_Q \to \infty$, the $Q\bar{q}$ reduced mass approaches the constant value $\mu \to m_q$, we expect that $\psi(0)$ itself approaches a constant in this limit,[4] and the scaling behavior $F_M \propto (m_M)^{-1/2}$ then follows immediately from Eq. (3.3). Alternatively, the dependence of F_M on m_M can be derived using the wavepacket formalism introduced in Chap. XII.

This quark model result can be validated in the heavy-quark limit [Ei 88]. Consider the contribution of meson M to the correlation function

$$C(t) = \int d^3x\ \langle 0\left|A_0(t,\mathbf{x})A_0^\dagger(0)\right|0\rangle, \tag{3.12}$$

where $A_0 \equiv \bar{q}\gamma_0\gamma_5 Q$. Inserting a complete set of intermediate states and isolating the contribution of meson M, we have

$$C(t) = \int d^3x \int \frac{d^3\mathbf{p}}{(2\pi)^3 2E_\mathbf{p}} \langle 0\,|A_0(t,\mathbf{x})|\,M(\mathbf{p})\rangle\langle M(\mathbf{p})\,|A_0(0)|\,0\rangle + \cdots, \tag{3.13}$$

where the ellipses denote other intermediate states. From the definition of F_M, one finds

$$C(t) = \frac{F_M^2 m_M^2}{2m_M} e^{-im_M t} + \cdots. \tag{3.14}$$

Alternatively, the heavy quark develops in time in this correlation function according to the static propagator of Eq. (XIII–3.6),

$$C(t) = -\frac{i}{2}\,e^{-im_Q t}\langle 0|\bar{q}(t,0)\gamma_0\gamma_5 P(t,0)(1+\gamma_5)\gamma_0\gamma_5 q(0)|0\rangle, \tag{3.15}$$

with all the dynamics being contained in the light degrees of freedom. The matrix element is independent of m_M, and the scaling behavior,

$$F_M \propto (m_M)^{-1/2}, \tag{3.16}$$

follows immediately. This technique is applicable to lattice theoretic calculations of F_M. There, one considers euclidean ($t \to -i\tau$) correlation functions, and identifies the M contribution by the $e^{-m_M\tau}$ behavior. At present, lattice calculations attempting to obtain physical results from the $m_Q \to \infty$ limit and from the light-quark limit do not agree in regions of overlap. We thus feel it is premature to quote

[4] For example, in the nonrelativistic potential model, the S-wave wavefunction at the origin is related to the reduced mass by $|\psi(0)|^2 = \mu\langle dV/dr\rangle/2\pi\hbar^2$.

theoretical values of F_D, F_B. Another piece of quark model lore which can be justified by this correlation function is that the mass difference $m_M - m_Q$ approaches a constant value in the $m_Q \to \infty$ limit. This can be inferred by comparing the exponential time dependences in Eq. (3.14) and Eq. (3.15), and noting that the difference must be be independent of the heavy quark.

The heavy-quark limit also makes predictions [IsW 89] for transition form factors between two heavy quarks (which for definiteness we shall call b and c). Recall the lagrangian developed in Eq. (XIII–3.15), the leading term of which is

$$\mathcal{L}_v = \bar{h}_v^{(c)} i v \cdot D\, h_v^{(c)} + \bar{h}_v^{(b)} i v \cdot D\, h_v^{(b)}. \tag{3.17}$$

This lagrangian exhibits an $SU(2)$-flavor symmetry involving rotation of $h_v^{(c)}$ and $h_v^{(b)}$. It is also spin-independent, and thus contains an additional $SU(2)$-spin symmetry. The two $SU(2)$s may be combined to form an $SU(4)$ flavor–spin invariance. Physically, the internal structure of hadrons containing a heavy quark and moving at a common velocity is seen to become independent of the quark flavor and spin. This property leads to many relations between transition amplitudes.

An example of a process appropriate for the heavy-quark technique is the weak semileptonic transition $B \to D$ induced by a vector current. For a static matrix element (i.e., both B and D at rest), the weak current transforms quark flavor $b \to c$, but leaves the remaining contents unchanged, resulting in unit wavefunction overlap. This can be seen calculationally by noting that the time component of the spatially integrated current is the conserved charge of the $SU(2)$-flavor group mentioned above,

$$\begin{aligned} \int d^3x\, \langle D(\mathbf{p}')\, | \bar{c}(x)\gamma_0 b(x) |\, \bar{B}(\mathbf{p})\rangle &= \delta(\mathbf{p}-\mathbf{p}')\, \sqrt{4 m_D m_B} \\ &= \delta(\mathbf{p}-\mathbf{p}')\, [f_+(t_m)\,(m_D+m_B) + f_-(t_m)\,(m_B-m_D)], \end{aligned} \tag{3.18}$$

where $t_m = (m_B - m_D)^2$ is the value of $t \equiv (p-p')^2$ at the point of zero recoil, and the general decomposition of a vector-current matrix element,

$$\langle D(\mathbf{p}') \left| \bar{c}\gamma_\mu b \right| \bar{B}(\mathbf{p})\rangle = f_+(t)\left(p+p'\right)_\mu + f_-(t)\left(p-p'\right)_\mu , \tag{3.19}$$

has been used in the second line of Eq. (3.18). We have seen results similar to Eq. (3.18) in the discussion of the Shifman–Voloshin limit in the previous section. However, there the restriction $m_B - m_D \ll m_B + m_D$ was required, whereas here no restriction is implied as long as both quarks are sufficiently heavy.

This framework may be extended to nonstatic transitions [IsW 90] with the observation that the heavy-quark symmetry can be applied in any frame moving

https://doi.org/10.1017/9781009291033.015 Published online by Cambridge University Press

at fixed velocity. First, in addition to Eq. (3.19) for the $B \to D$ transition, we require also the $D \to D$ and $B \to B$ vector form factors,

$$\langle D(\mathbf{p}'_D) \left|\bar{c}\gamma_\mu c\right| D(\mathbf{p}_D)\rangle = f_D(t_D)\left(p_D + p'_D\right)_\mu ,$$
$$\langle \bar{B}(\mathbf{p}'_B) \left|\bar{b}\gamma_\mu b\right| \bar{B}(\mathbf{p}_B)\rangle = f_B(t_B)\left(p_B + p'_B\right)_\mu , \tag{3.20}$$

where $f_B(0) = f_D(0) = 1$. Considering the momentum transfers t_D, t_B, and $t_{BD} \equiv (p_B - p'_D)^2$ in terms of the velocities, using $p_j^\mu = m_j v^\mu$, $\mathbf{p}_B = m_B\mathbf{v}$, and $\mathbf{p}_D = m_D\mathbf{v}$, we have

$$t_B = \left(p_B - p'_B\right)^2 = 2m_B^2\left(1 - v\cdot v'\right),$$
$$t_D = \left(p_D - p'_D\right)^2 = 2m_D^2\left(1 - v\cdot v'\right),$$
$$t_{BD} = (p_B - p_D)^2 = (m_B - m_D)^2 + 2m_Bm_D\left(1 - v\cdot v'\right). \tag{3.21}$$

If each transition has common velocity factors, the various momentum transfers are related by

$$t_D = \frac{m_D^2}{m_B^2}t_B = \frac{m_D}{m_B}\left(t_{BD} - t_m\right). \tag{3.22}$$

In view of the normalization convention of Eq. (3.2), one must divide the state vector of particle i by $\sqrt{2m_i}$ (assuming $m_i \gg |\mathbf{p}|$) before applying the $b \leftrightarrow c$ symmetry. Upon doing so and requiring the resulting expressions to be identical functions of the velocities $\mathbf{v}$ and $\mathbf{v}'$ leads to the relations

$$\frac{\langle D(\mathbf{p}'_D) \left|\bar{c}\gamma_i c\right| D(\mathbf{p}_D)\rangle}{2m_D} = \frac{\langle \bar{B}(\mathbf{p}'_B) \left|\bar{b}\gamma_i b\right| \bar{B}(\mathbf{p}_B)\rangle}{2m_B} = \frac{\langle D(\mathbf{p}_D)' \left|\bar{c}\gamma_i b\right| \bar{B}(\mathbf{p}_B)\rangle}{\sqrt{4m_Dm_B}},$$
$$f_D(t_D)\frac{\left(\mathbf{v}+\mathbf{v}'\right)_i}{2} = f_B(t_B)\frac{\left(\mathbf{v}+\mathbf{v}'\right)_i}{2} = f_+(t_{BD})\frac{\left(m_B\mathbf{v}+m_D\mathbf{v}'\right)_i}{\sqrt{4m_Dm_B}}$$
$$+ f_-(t_{BD})\frac{\left(m_B\mathbf{v}-m_D\mathbf{v}'\right)_i}{\sqrt{4m_Dm_B}}. \tag{3.23}$$

After simple algebra, this results in the form-factor relations

$$f_B(t) = f_D\left[\frac{m_D^2}{m_B^2}t\right],$$
$$f_+(t) = \frac{m_B + m_D}{\sqrt{4m_Bm_D}}f_D\left[\frac{m_D}{m_B}(t - t_m)\right],$$
$$f_-(t) = -\frac{m_B - m_D}{\sqrt{4m_Bm_D}}f_D\left[\frac{m_D}{m_B}(t - t_m)\right]. \tag{3.24}$$

Although consistent with Eq. (3.21), this manages to separate out $f_\pm$. The results are expressible in terms of a single function of velocity. It is notationally simpler to express the kinematic dependence using $v \cdot v'$ instead of t, i.e., $f_i(t) \to f_i(v \cdot v')$. Thus, we have

$$f_B(v \cdot v') = f_D(v \cdot v') = \sqrt{\frac{4m_B m_D}{m_B + m_D}} f_+(v \cdot v'),$$
$$= -\sqrt{\frac{4m_B m_D}{m_B - m_D}} f_-(v \cdot v') \equiv \xi(v \cdot v'), \quad (3.25)$$

where, aside from the constraint $\xi(1) = 1$, the function $\xi(v \cdot v')$ is unknown and must thus be determined phenomenologically. If we exploit the full $SU(4)$-flavor–spin symmetry, then all the weak-current form factors involving B, B^*, D, and D^* can be expressed in terms of the quantity $\xi(v \cdot v')$, e.g.,

$$\langle D^*(\mathbf{p}'_D) \left| \bar{c}\gamma_\mu b \right| \bar{B}(\mathbf{p}_B)\rangle = i\sqrt{m_{D^*} m_B}\xi(v \cdot v')\epsilon_{\mu\nu\alpha\beta}\epsilon^*_\nu(\mathbf{p}'_D)v'_\alpha v_\beta,$$
$$\langle D^*(\mathbf{p}'_D) \left| \bar{c}\gamma_\mu\gamma_5 b \right| \bar{B}(\mathbf{p}_B)\rangle = \sqrt{m_{D^*} m_B}\xi(v \cdot v')\left[(1 + v \cdot v')\epsilon^*_\mu - \epsilon^* \cdot v\, v'_\mu.\right] \quad (3.26)$$

The symmetry language is appropriate here because, similar to the symmetry relations detailed in the first part of this book, we have *related* different processes even though there remains an uncalculated ingredient to be determined from experiment. However, effective field theory techniques allow a more detailed study of the same matrix elements beyond just the leading symmetry relation. Hard perturbative effects can also be included [Wi 91, CzM 97]. Suppressed corrections due to deviations from the heavy-quark limit can be calculated in the effective theory. The shape of the form factors [CaLN 98] can be determined experimentally, but what is most important phenomenologically is the normalization of these form factors at the zero-recoil point $v \cdot v' = 1$. This deviation is second order in the inverse masses [Lu 90] which, since $m_c \ll m_b$, means that it is of order $1/m_c^2$. While analytic estimates of this deviation can be achieved [ShUV 95, GaMU 12], lattice methods now can provide well-controlled calculations of this effect [Be *et al.* 09].

For the $b \to u$ semileptonic transition, there is no corresponding heavy-quark theory that provides a solid starting point for analysis of the $B \to \pi e \nu$ decay. Quark model calculations are particularly unreliable for this transition. Fortunately, improved lattice calculations now appear capable of calculating the transition matrix element in the region of small recoil [DaGWDLS 06, Ba *et al.* 09]. Supplemented by theoretical constraints [BeH 06], experimental work can measure the q^2 variation and use the lattice matrix element to provide the normalization when using this process to measure $V_{\rm ub}$.

Phenomenologically, exclusive decays are key ingredients to the extraction of the CKM elements. The present best values from exclusive decays are [RPP 12]:

$$V_{\rm cb} = (39.6 \pm 0.9) \times 10^{-3}, \qquad V_{\rm ub} = (3.23 \pm 0.31) \times 10^{-3}. \tag{3.27}$$

The reader will note there is a modest disagreement between the values of these elements between the inclusive determination of Eq. (2.17) and the exclusive values of Eq. (3.27). For $V_{\rm ub}$, the effect is sizeable and may be indicative of a gap in our theoretical methods. The smaller disagreement seen in $V_{\rm cb}$ may also be an indication that more theoretical work is needed at understanding the duality between inclusive and exclusive methods.

XIV–4 B^0–$\bar{B}^0$ and D^0–$\bar{D}^0$ mixing

Just as $K^0-\bar{K}^0$ mixing occurs due to the weak interactions, so does mixing exist in the $B_d-\bar{B}_d$, $B_s-\bar{B}_s$ and $D^0-\bar{D}^0$ systems. We shall discuss first the $B_d-\bar{B}_d$ and $B_s-\bar{B}_s$ mixings, then conclude with the D^0 case. The formalism is the same in all situations and can be taken directly from the discussion of $K^0-\bar{K}^0$ mixing in Sect. IX–1.

B^0–$\bar{B}^0$ mixing

The mixing occurring in B_d and B_s mesons is short-distance dominated. This is because (i) the dominant weak coupling of the b quark is to the t quark, and (ii) the short-distance box diagram (Fig. XIV–2) grows roughly with the squared-mass of the intermediate-state quarks. Since the very heavy mass of the top quark greatly enhances its contribution, the top intermediate state dominates B-meson mixing.

The effective hamiltonians for B_d, and B_s mixing are[5]

$$\begin{aligned}
\mathcal{H}_{\rm W}^{\Delta B_d=2} &= \frac{G_F^2}{16\pi^2}\left(V_{\rm tb}V_{\rm td}^*\right)^2 m_t^2 H(x_t)\eta_B O^{B_d} + \text{h.c.},\\
\mathcal{H}_{\rm W}^{\Delta B_s=2} &= \frac{G_F^2}{16\pi^2}\left(V_{\rm tb}V_{\rm ts}^*\right)^2 m_t^2 H(x_t)\eta_B O^{B_s} + \text{h.c.},\\
O^{B_d} &= \bar{d}\gamma_\mu(1+\gamma_5)b\,\bar{d}\gamma^\mu(1+\gamma_5)b,\\
O^{B_s} &= \bar{s}\gamma_\mu(1+\gamma_5)b\,\bar{s}\gamma^\mu(1+\gamma_5)b,
\end{aligned} \tag{4.1}$$

where $\eta_B \simeq 0.9$ is the QCD correction and $H(x_t)$ is given in Eq. (IX–1.20). The matrix elements of O^{B_d} and O^{B_s} can be parameterized analogously to that used in kaon mixing,

$$\langle B_d \left| O^{B_d} \right| \bar{B}_d\rangle = \frac{16}{3}F_{B_d}^2 m_{B_d}^2 B_{B_d}, \qquad \langle B_s \left| O^{B_s} \right| \bar{B}_s\rangle = \frac{16}{3}F_{B_s}^2 m_{B_s}^2 B_{B_s}, \tag{4.2}$$

[5] A more advanced treatment of B_s–$\bar{B}_s$ mixing than given here appears in [LeN 07].

https://doi.org/10.1017/9781009291033.015 Published online by Cambridge University Press

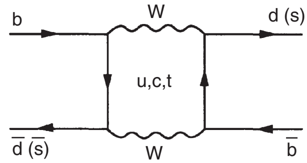

Fig. XIV–2 Box diagram contribution to B-meson mixing.

where the pseudoscalar decay constants are normalized as

$$\langle 0 \left| \bar{d}\gamma^\mu\gamma_5 b \right| \bar{B}_d(\mathbf{p})\rangle = i\sqrt{2}\, F_{B_d} p^\mu, \qquad \langle 0 \left| \bar{s}\gamma^\mu\gamma_5 b \right| \bar{B}_s(\mathbf{p})\rangle = i\sqrt{2}\, F_{B_s} p^\mu. \quad (4.3)$$

These correspond to the normalization $F_\pi \simeq 92$ MeV.

Both B_d and B_s mixing have been observed, with the results,[6]

$$x_d \equiv \frac{\Delta m_{B_d}}{\Gamma_{B_d}} = 0.775 \pm 0.006, \qquad x_s \equiv \frac{\Delta m_{B_s}}{\Gamma_{B_s}} = 26.82 \pm 0.23. \quad (4.4)$$

The width difference of B_d is consistent with zero, while that of B_s is nonzero but small,

$$\frac{\Delta\Gamma_d}{\Gamma_d} = 0.015 \pm 0.018, \qquad \frac{\Delta\Gamma_s}{\Gamma_s} = 0.123 \pm 0.017. \quad (4.5)$$

In Eqs. (4.4)–(4.5) above, we have denoted $\Delta m \equiv m_H - m_L$ and $\Delta\Gamma \equiv \Gamma_H - \Gamma_L$, where H (L) refers to the heavier (lighter) of the neutral B CP eigenstates,

The large magnitude of x_s/x_d is readily understood in the Standard Model to be mainly due to the CKM elements, as the ratio is predicted to be

$$\frac{\Delta m_{B_s}}{\Delta m_{B_d}} = \left[\frac{F_{B_s}^2 B_{B_s}}{F_{B_d}^2 B_{B_d}}\right] \left|\frac{V_{\text{ts}}}{V_{\text{td}}}\right|^2. \quad (4.6)$$

The $SU(3)$ breaking in the matrix elements is well under control in lattice calculations [LaLV 10],

$$\frac{F_{B_s}\sqrt{B_{B_s}}}{F_{B_d}\sqrt{B_{B_d}}} = 1.237 \pm 0.032. \quad (4.7)$$

The remaining dependence in the ratio of the mass splittings comes from the CKM elements and in fact this ratio is the most precise measurement of the relative sizes of these CKM elements

$$\left|\frac{V_{\text{ts}}}{V_{\text{td}}}\right| = 4.739 \pm 0.126, \quad (4.8)$$

consistent with other determinations. This is an important test of the Standard

[6] We use the updated version of [Am *et al.* (Heavy Flavor Averaging Group collab.) 12] found in www.slac.stanford.edu/xorg/hfag.

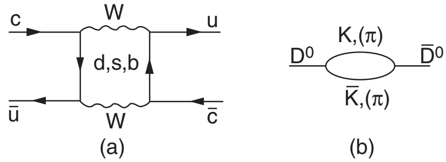

Fig. XIV–3 Short-distance (a) and long-distance (b) contributions to D-meson mixing.

Model as New Physics could readily contribute to Δm_{B_d} and/or Δm_{B_s}. The absolute magnitudes of these mixings are also compatible with the Standard Model. Using the mixing formula developed in Chap. IX and the lattice magnitude [LaLV 10] $F_{B_d}\sqrt{B_{B_d}} = (149 \pm 9)$ MeV, the experimental number for Δm_d is reproduced with $|V_{\rm td}| = (8.4 \pm 0.6) \times 10^{-3}$, which becomes a tight constraint on fits of the unitarity triangle, to be discussed shortly.

The width differences are smaller than the mass differences because real on-shell intermediate states are required; thus, top-quark intermediate states do not contribute to $\Delta\Gamma_{d,s}$. For this reason, the widths $\Delta\Gamma_{d,s}$ are suppressed compared to $\Delta m_{d,s}$ by a factor of roughly m_b^2/m_t^2. The width difference for B_d is smaller than that for B_s because the CKM favored decay mechanism $b \to c\bar{c}s$ when active for a $b\bar{d}$ meson leads to an intermediate state ($c\bar{c}s\bar{d}$) that cannot convert to a $d\bar{b}$ meson, while when occurring in the decay of $b\bar{s}$ leads to intermediate states ($c\bar{c}s\bar{s}$ or $c\bar{c}$) that can transition back to $s\bar{b}$. Thus, $\Delta\Gamma_d$ is CKM-suppressed compared to $\Delta\Gamma_s$. The measurements of $\Delta\Gamma_{d,s}$ are also compatible with theoretical expectations [LeN 07].

D^0–$\bar{D}^0$ *mixing*

The analysis of D^0–$\bar{D}^0$ transitions is considerably more complex than that involving $B_{d,s}$ mesons because the mixing is *not* short-distance-dominated [Wo 85, DoGH 86*a*]. To see this, we display the corresponding box diagram in Fig. XIV–3(a), and some possible long-distance contributions in Fig. XIV–3(b). The GIM cancelation in the intermediate state is between the two light quarks d, s (the b-quark contribution is suppressed by CKM angles). However, there is no compensating large mass factor here; long-distance and short-distance effects contribute at the same order of magnitude. As a result, reliable *quantitative* predictions of Δm_D have eluded theorists thus far, despite the attempts of many to solve the problem. Even such basic issues as correctly predicting the sign of Δm_D or determining to what extent a component from New Physics could be present [GoHPP 07] remain unresolved.

https://doi.org/10.1017/9781009291033.015 Published online by Cambridge University Press

For example, consider the application of the OPE (which has worked so well for $B_{d,s}$ mixings) to D^0 mixing [Ge 92, OhRS 93, BiU 01, BoLRR 10],

$$\langle \bar{D}^0|\mathcal{H}_{|\Delta C|=2}|D^0\rangle = G\sum_i \mathcal{C}_i(\mu)\langle \bar{D}^0|\mathcal{Q}_i|D^0\rangle, \tag{4.9}$$

where the prefactor G has the unit of inverse squared mass, the sum is over operator dimension, and both Standard Model and New Physics operators are included. The expansion begins at dimension six, with two operators for just the Standard Model and eight upon including New Physics. However, even within just the Standard Model, the number of operators increases sharply as the dimension grows, e.g., there are about a dozen at dimension nine and more than twenty at dimension twelve. This introduces a multitude of unknown parameters. It is also the case that the sum in Eq. (4.9) is not expected to converge rapidly because the ratio $\Lambda_{QCD}/m_c \simeq 0.25$ is not sufficiently small.

Some aspects of $D^0-\bar{D}^0$ mixing can, however, be understood. For example, the Standard Model clearly requires that $\Delta m_D/\Gamma_D \ll 1$ because Δm_D is twice Cabibbo-suppressed (i.e. $\Delta m_D = \mathcal{O}(\lambda^2)$) while Γ_D suffers no such suppression. Hence, upon counting CKM factors and noting that the *GIM* cancelation is a measure of the breaking of $SU(3)$ symmetry, one is led to estimate that[7]

$$\frac{\Delta m_D}{\Gamma_D} \sim \lambda^2 \times [SU(3)\,\text{breaking}] = \mathcal{O}(10^{-2}). \tag{4.10}$$

Of the various meson-mixing systems, the $D^0-\bar{D}^0$ transitions were the last to be detected experimentally. However, by studying the decay time dependence of $D^0 \to K^+\pi^-/D^0 \to K^-\pi^+$, a recent experiment [Aa *et al.* (LHCb collab.) 13*a*] excludes the no-mixing hypothesis with a probability of over nine standard deviations. The current-mixing values in [RPP 12] are

$$x_D \equiv \frac{\Delta m_D}{\Gamma_D} = \left(0.63^{+0.19}_{-0.20}\right) \times 10^{-2}, \qquad \frac{\Delta\Gamma_D}{\Gamma_D} = (1.50 \pm 0.24) \times 10^{-2}. \tag{4.11}$$

The suppression in $D^0-\bar{D}^0$ mixing is evident upon comparing the above value for x_D with those for x_d and x_s in Eq. (4.4).

Observation of D^0–$\bar{D}^0$ mixing motivates the search for *CP* violation in the *D*-meson system. Here, we cite two recent results. In one, the *CP*-violating asymmetry A_D in the time dependent transition $D^0 \to K^+\pi^-$ is measured to be $A_D = (-0.7 \pm 1.9)\,\%$, which is consistent with zero [Aa *et al.* (LHCb collab.) 13*c*]. In the other, the *CP*-violating asymmetry $A_\Gamma(f)$, between the D^0 and $\overline{D}^0$ decay rates to a given final state f, yields results also consistent with zero [Aa *et al.* (LHCb collab.) 13*d*],

[7] Actually, it can be proved that if $SU(3)$ violation in D^0 mixing enters perturbatively, then a group theoretic analysis of $\langle 0|D\mathcal{H}_{\rm w}\mathcal{H}_{\rm w}D|0\rangle$ shows that $SU(3)$ breaking occurs only at second order [FaGLP 02].

https://doi.org/10.1017/9781009291033.015 Published online by Cambridge University Press

$$A_\Gamma(\pi^+\pi^-) = (0.33 \pm 1.06 \pm 0.14) \times 10^{-3},$$
$$A_\Gamma(K^+K^-) = (-0.35 \pm 0.62 \pm 0.12) \times 10^{-3}. \qquad (4.12)$$

The uncertainties in the above determinations are dominated by statistical, rather than by systematic, effects. Thus, although the current status of *CP* violation in charm is inconclusive, there is reason to be optimistic that additional statistics as obtained in forthcoming studies will yield nonzero results.

XIV–5 The unitarity triangle

The B-meson transitions form a nontrivial system and provide much of our information on the pattern of weak mixing. The overall B lifetime and $b \to c$ semileptonic decays are governed by $V_{\rm cb}$, the suppressed $b \to u$ modes by $V_{\rm ub}$, $B_d - \bar{B}_d$ mixing by $V_{\rm td}$, and $B_s - \bar{B}_s$ mixing by $V_{\rm ts}$. Together with the $V_{\rm us}$ element, these form all of the 'interesting' sectors of weak mixing.

There is a useful pictorial representation of the constraints of unitarity on these elements. Consider the effect of the unitarity relation

$$V_{\rm ub}V_{\rm ud}^* + V_{\rm cb}V_{\rm cd}^* + V_{\rm tb}V_{\rm td}^* = 0. \qquad (5.1)$$

Of the components to this equation, $V_{\rm ud}$, $V_{\rm td}$ and $V_{\rm cd}$ are known up to corrections of second order in $\lambda = |V_{\rm us}|$, yielding

$$V_{\rm ub} - \lambda V_{\rm cb} + V_{\rm td}^* = 0. \qquad (5.2)$$

If we treat these elements as complex vectors, this relation is equivalent to a triangle in the complex plane. In the Wolfenstein parameterization the various elements are

$$V_{\rm cb} = -V_{\rm ts} = A\lambda^2, \quad V_{\rm ub} = \lambda^2 A(\rho - i\eta), \quad V_{\rm td} = \lambda^3 A(1 - \rho - i\eta). \qquad (5.3)$$

The unitarity triangle is shown in Fig. XIV–4. Note that the unitarity triangle can be constructed knowing only the *magnitude* of the elements $|V_{\rm cb}|$, $|V_{\rm ub}|$, and $|V_{\rm td}|$. The existence of such a closed triangle is independent of the parameterization. Other unitarity triangles, corresponding to the other unitarity constraints, also exist but are either less useful than this one or are equivalent to it [Ja 89].

The unitarity triangle has an important connection with *CP* violation. If the *CP*-violating parameter η vanishes, the triangle is reduced down to a line since all the angles go to either 0° or 180°. In fact, the area $\lambda^6 A^2 \eta$ of this triangle is exactly the unique rephasing invariant measure of *CP* violation. The angles $\alpha,\ \beta,\ \gamma$ are themselves indicators of nonconservation of *CP* and play a role in the B studies to be described in the next section.[8] Note that the magnitudes of the sides of the

[8] In the literature there is an alternate naming of angles $\varphi_1 = \beta, \varphi_2 = \alpha, \varphi_3 = \gamma$. We are following the conventions of the Particle Data Group.

https://doi.org/10.1017/9781009291033.015 Published online by Cambridge University Press

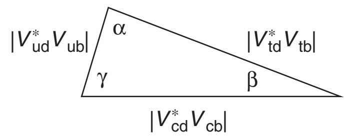

Fig. XIV–4 The unitarity triangle.

triangle and the interior angles of the triangle are all independently measurable and the fact that the separate measurements are consistent is a powerful test of the Standard Model. Our Fig. XIV–4 is drawn using the present fits of the sides and angles, and illustrates the relative magnitudes of these elements.

XIV–6 *CP* violation in *B*-meson decays

The decays of B mesons exhibit a rich variety of CP-violating signals, some of which are rather large [BiS 81]. These reactions have provided dramatic confirmation of the validity of the CKM mixing scheme as the dominant origin of CP violation. Recall that the value of ϵ cannot be regarded as a prediction of the Standard Model because there is an unknown parameter, the CKM phase δ, which must be adjusted to fit experiment. The value of ϵ'/ϵ is consistent with the Standard Model and is an important verification of the existence of direct CP violation, but theoretical uncertainties are presently too large for this to be a precision test. However, the Standard Model, with its single CP-odd parameter, makes clear predictions for the patterns of CP violations in B decays, and observation has confirmed many of these.

There is an important division in the study of CP violations for B mesons: (i) processes which proceed via $B^0-\bar{B}^0$ mixing, and (ii) those which do not. We shall discuss those involving mixing first, and then return to those not related to mixing.

CP-odd signals induced by mixing

General formalism: The analysis of time evolution for a B^0 or $\bar{B}^0$ meson parallels that of a neutral kaon. Given the conventions for Δm and $\Delta\Gamma$ following Eq. (4.5), one obtains for states that start out at $t = 0$ being either B^0 or $\bar{B}^0$,

$$|B^0(t)\rangle = g_+(t)|B^0\rangle + \frac{q}{p}g_-(t)|\bar{B}^0\rangle,$$
$$|\bar{B}^0(t)\rangle = \frac{p}{q}g_-(t)|B^0\rangle + g_+(t)|\bar{B}^0\rangle,$$

https://doi.org/10.1017/9781009291033.015 Published online by Cambridge University Press

$$\frac{p}{q} \equiv \sqrt{\frac{M_{12} - i\Gamma_{12}}{M_{12}^* - i\Gamma_{12}^*}},$$

$$g_\pm(t) \equiv \frac{1}{2} e^{-\Gamma_L t/2} e^{i m_L t} \left[1 \pm e^{-\Delta\Gamma t/2} e^{i\Delta m t}\right]. \tag{6.1}$$

The strategy for observing *CP*-violating asymmetries is to compare the decay $B^0(t) \to f$, where f is some given final state, to that of $\bar{B}^0(t) \to \bar{f}$, where $\bar{f}$ is the *CP*-conjugate of f,

$$|\bar{f}\rangle = \mathcal{CP}|f\rangle. \tag{6.2}$$

Let us define the matrix elements

$$\begin{aligned} A(f) &= \langle f|\mathcal{H}_W|B^0\rangle, \qquad & \bar{A}(\bar{f}) &= \langle \bar{f}|\mathcal{H}_W|\bar{B}^0\rangle, \\ \bar{A}(f) &= \langle f|\mathcal{H}_W|\bar{B}^0\rangle, \qquad & A(\bar{f}) &= \langle \bar{f}|\mathcal{H}_W|B^0\rangle, \end{aligned} \tag{6.3}$$

and their ratios,[9]

$$\bar{\rho}(f) = \frac{\bar{A}(f)}{A(f)}, \qquad \rho(\bar{f}) = \frac{A(\bar{f})}{\bar{A}(\bar{f})}. \tag{6.4}$$

The decay rates for the two processes are easily found to be [BiKUS 89]

$$\begin{aligned} \Gamma_{B^0(t)\to f} &\propto \left[a + b e^{-\Delta\Gamma t} + c\, e^{-\frac{1}{2}\Delta\Gamma t}\cos\Delta m\, t + d\, e^{-\frac{1}{2}\Delta\Gamma t}\sin\Delta m\, t\right] e^{-\Gamma_L t}, \\ a &= |A(f)|^2 \left(\frac{1}{2}\left[1 + \left|\frac{q}{p}\bar{\rho}(f)\right|^2\right] + \mathrm{Re}\left[\frac{q}{p}\bar{\rho}(f)\right]\right), \\ b &= |A(f)|^2 \left(\frac{1}{2}\left[1 + \left|\frac{q}{p}\bar{\rho}(f)\right|^2\right] - \mathrm{Re}\left[\frac{q}{p}\bar{\rho}(f)\right]\right), \\ c &= |A(f)|^2 \left(1 - \left|\frac{q}{p}\bar{\rho}(f)\right|^2\right), \\ d &= 2\,|A(f)|^2\, \mathrm{Im}\left[\frac{q}{p}\bar{\rho}(f)\right], \end{aligned} \tag{6.5a}$$

and

$$\begin{aligned} \Gamma_{\bar{B}^0(t)\to \bar{f}} &\propto \left[\bar{a} + \bar{b}\, e^{-\Delta\Gamma t} + \bar{c}\, e^{-\frac{1}{2}\Delta\Gamma t}\cos\Delta m\, t + \bar{d}\, e^{-\frac{1}{2}\Delta\Gamma t}\sin\Delta m\, t\right] e^{-\Gamma_L t}, \\ \bar{a} &= |\bar{A}(\bar{f})|^2 \left(\frac{1}{2}\left[1 + \left|\frac{p}{q}\rho(\bar{f})\right|^2\right] + \mathrm{Re}\left[\frac{p}{q}\rho(\bar{f})\right]\right), \end{aligned}$$

[9] We caution the reader not to confuse the notation for these ratios with the CKM element ρ in the Wolfenstein parameterization of Eq. (II–4.19).

https://doi.org/10.1017/9781009291033.015 Published online by Cambridge University Press

$$\bar{b} = \left|\bar{A}(\bar{f})\right|^2 \left(\frac{1}{2}\left[1 + \left|\frac{p}{q}\rho(\bar{f})\right|^2\right] - \mathrm{Re}\left[\frac{p}{q}\rho(\bar{f})\right]\right),$$
$$\bar{c} = \left|\bar{A}(\bar{f})\right|^2 \left(1 - \left|\frac{p}{q}\right|^2 \rho(\bar{f})|^2\right),$$
$$\bar{d} = 2\left|\bar{A}(\bar{f})\right|^2 \mathrm{Im}\left[\frac{p}{q}\rho(\bar{f})\right]. \tag{6.5b}$$

Any observed difference between these two quantities would indicate the presence of *CP* violation.

Before considering some examples, there is a simplifying approximation which it is useful to make. As seen in the previous section $M_{12} \gg \Gamma_{12}$ for B and B_s, so it is a good approximation to neglect Γ_{12} (and hence $\Delta\Gamma$) in almost all cases.[10] In this approximation q/p becomes a pure phase, $q/p = e^{i\varphi}$, so that $|q/p| = 1$.

Decays to CP eigenstates

The most striking processes are those where the final state f is a *CP* eigenstate, $|\bar{f}\rangle = \pm|f\rangle$, such as $f = \psi K_S, \psi K_L, D^+D^-, \pi^+\pi^-$. In this case one has $\bar{\rho}(f) = 1/\rho(\bar{f})$. Time-dependent *CP* asymmetries have two components

$$A_f(t) = \frac{\Gamma(\bar{B}^0(t) \to f) - \Gamma(B^0(t) \to f)}{\Gamma(\bar{B}^0(t) \to f) + \Gamma(B^0(t) \to f)} = S_f \sin(\Delta m t) - C_f \cos(\Delta m t), \tag{6.6}$$

where

$$S_f = \frac{2\mathrm{Im}\left[\frac{q}{p}\bar{\rho}(f)\right]}{1 + \left|\frac{q}{p}\bar{\rho}(f)\right|^2}, \qquad C_f = \frac{1 - \left|\frac{q}{p}\bar{\rho}(f)\right|^2}{1 + \left|\frac{q}{p}\bar{\rho}(f)\right|^2)}. \tag{6.7}$$

We see that there are two possible ways that the asymmetry can be nonvanishing, corresponding to the S_f and C_f amplitudes.

The cleanest analysis occurs when $|\bar{\rho}(f)| = 1$, i.e., $|\bar{A}(f)| = |A(f)|$. An example is $B_d \to \psi K_s^0$, which proceeds dominantly through $b \to c\bar{c}s$, so that both factors are pure phases

$$\bar{\rho}(f) = \frac{V_{\mathrm{cs}}^* V_{\mathrm{cb}}}{V_{\mathrm{cs}} V_{\mathrm{cb}}^*}, \qquad \frac{q}{p} = \frac{V_{\mathrm{td}} V_{\mathrm{tb}}^*}{V_{\mathrm{td}}^* V_{\mathrm{tb}}}. \tag{6.8}$$

[10] The one exception is the semileptonic asymmetry to be discussed below.

https://doi.org/10.1017/9781009291033.015 Published online by Cambridge University Press

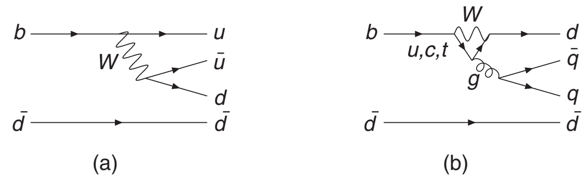

Fig. XIV–5 Tree (a) and penguin (b) diagrams for $B \to \pi\pi$.

In this case, it is clear that $C_{\psi K} = 0$. The asymmetry involves the relative phases of $V_{\rm cs}^* V_{\rm cb}$ and $V_{\rm td}^* V_{\rm tb}$, which we see from Fig. XIV–4 is the angle β, such that the result becomes

$$S_{\psi K} = \sin 2\beta. \tag{6.9}$$

This prediction is independent of hadronic uncertainties and depends only on the phases in the CKM matrix. The result is large, with the resulting measurement [RPP 12] of the angle β of $\sin 2\beta = 0.679 \pm 0.020$, consistent with other constraints on the unitarity triangle. *CP* violation in this mode is one of the cleanest and most direct confirmations of the Standard Model.

One might at first expect that $|\bar{\rho}(f)|^2 = 1$ is automatic if f is a *CP* eigenstate. However, it is possible to obtain $|\bar{\rho}(f)| \neq 1$ if there are two different ways to reach the same final state. For example, one could have the decay $\bar{B}^0 \to \pi^+\pi^-$ either directly through $b \to u\bar{u}d$ or through the penguin diagram, which includes the CKM elements for c or t intermediate states, cf. Fig. XIV–5.[11] By CKM unitarity, we have $V_{\rm cb}^* V_{\rm cd} = -(V_{\rm ub}^* V_{\rm ud} + V_{\rm tb}^* V_{\rm td})$. Therefore, if we absorb the portion of the penguin diagram proportional to $V_{\rm ub}^* V_{\rm ud}$ into the tree-amplitude reduced matrix element, which carries the same CKM factor, we have the amplitude expressed in terms of two CKM elements,

$$\begin{aligned} \bar{A}(\pi^+\pi^-) &= V_{\rm ud}^* V_{\rm ub}\,|T|\,e^{i\delta_T} + V_{\rm td}^* V_{\rm tb}\,|P|\,e^{i\delta_P}\ , \\ A(\pi^+\pi^-) &= V_{\rm ud} V_{\rm ub}^*\,|T|\,e^{i\delta_T} + V_{\rm td} V_{\rm tb}^*\,|P|\,e^{i\delta_P}, \end{aligned} \tag{6.10}$$

where T and P are tree and penguin amplitudes and $\delta_T,\ \delta_P$ are strong-interaction phase shifts. Because the weak phases change sign under *CP* and the strong phases do not, we have the ratio of amplitudes $|\bar{\rho}(f)| \neq 1$. Indeed, experimentally one finds

$$S_{\pi^+\pi^-} = -0.65 \pm 0.07, \qquad C_{\pi^+\pi^-} = -0.38 \pm 0.06, \tag{6.11}$$

[11] In discussions such as this, it is understood that the weak hamiltonian receives *QCD* radiative corrections, which can mix operators with identical quantum numbers. However, since we are using only the CKM factors and symmetry properties of the amplitudes, these corrections do not influence the analysis and are absorbed into the reduced matrix elements.

Table XIV–1. *Standard Model pattern for CP violation in B decays.*

Transitions	Examples	Im $(q/p)\bar{\rho}(f)^a$
$b \to c\bar{c}s$	$B_d \to \psi K_S$	$\sin 2\beta$
	$B_s \to \psi\varphi$	~ 0
$b \to c\bar{c}d$	$B_d \to D\bar{D}$	$\sin 2\beta$
	$B_s \to \psi K_S$	~ 0
$b \to u\bar{u}d$	$B_d \to \pi^+\pi^-$	$\sin 2\alpha$
	$B_s \to \pi^0 K_S$	$\sin 2\alpha$
$b \to u\bar{u}s$	$B_d \to \pi^0 K_S$	$\sin 2\alpha$
	$B_s \to \pi^0\varphi^0$	$\sin 2\gamma$

[a]The angles $\alpha,\ \beta,\ \gamma$ are defined by the unitarity triangle of Fig. XIV–4 and we take $|\bar{\rho}(f)| = 1$.

indicating the presence of both *CP*-violating phases and sizeable strong rescattering phases. The solution to this 'penguin pollution' involves looking at other $\pi\pi$ modes. There is an isospin relation among the three-pion channels (cf. Eq. (VIII–4.1)

$$A(\pi^+\pi^-) - A(\pi^0\pi^0) = \sqrt{2}A(\pi^+\pi^0), \tag{6.12}$$

similar to the kaon decay analysis of Chap. VIII. The penguin amplitude is purely $\Delta I = 1/2$ and hence only the tree amplitude can contribute to the $I = 2$ final state $\pi^\pm\pi^0$. Measurement of branching ratios and *CP* asymmetries $S_{\pi\pi}$, $C_{\pi\pi}$ allows one to disentangle the *CP* violation due to tree and penguin amplitudes [GrL 90]. For the tree amplitude, involving $V^*_{\rm ub}V_{\rm ud}$, the interference is with the B_d-mixing amplitude, dominated by the top quark, so that the measurement is of the CKM phase α.

At this stage we can categorize the decays of neutral B mesons to *CP* eigenstates. For this purpose it is most convenient to use the Wolfenstein form of the CKM matrix. In this parameterization, the elements $V_{\rm tb}$, $V_{\rm cb}$, $V_{\rm ts}$, $V_{\rm cs}$ are all almost purely real. The B_d and B_s decays can proceed either through the CKM-favored transition $b \to c\bar{c}s$ or the CKM-suppressed transitions $b \to u\bar{u}d$, $b \to c\bar{c}d$, $b \to u\bar{u}s$. In the former category are included $B_d \to \psi K_S$ and also $B_s \to \psi\varphi,\ \psi\eta,\ D_s^+ D_s^-$. The B_s decays pick up no phase since

$$\frac{q}{p} = \frac{V_{\rm ts}V^*_{\rm tb}}{V^*_{\rm ts}V_{\rm tb}} = 1 \ \ \text{and} \ \ \bar{\rho}(f) = \frac{V_{\rm cb}}{V^*_{\rm cb}} = 1 \ \Rightarrow \text{Im}\left[\frac{q}{p}\bar{\rho}(f)\right] = 0. \tag{6.13}$$

However, the B_d decay does pick up a phase, leading to a distinctive signature of the Standard Model. The CKM-suppressed decays can also be analyzed in terms of the angles which appear in the unitarity triangle, and are given in Table XIV–1 for the case $|\bar{\rho}(f)| = 1$. However, in some cases we know that $|\bar{\rho}(f)| \neq 1$, such that further efforts are required to extract the given angle, as described for the $\pi\pi$ system above. It should also be pointed out that under all circumstances, asymmetries for B_s are more difficult to observe because x_s is large due to the rapid oscillations in the $B_s \leftrightarrow \bar{B}_s$ system. Thus, regardless of whether one starts out at $t = 0$ with B_s or $\bar{B}_s$, after a few oscillation lengths one will have roughly equal amounts of B_s and $\bar{B}_s$.

Decays to non-CP eigenstates

There may also exist *CP* violation in final states which are *not CP* eigenstates. Consider, for example, the final state $B_d \to \pi^- K^+$. This transition can occur both through tree amplitudes, with the CKM factor $V_{\rm ub}^* V_{\rm us}$ and through penguin decays of the form $b \to s\bar{q}q$. Because the CKM elements satisfy $V_{\rm tb}^* V_{\rm ts} = -(V_{\rm cb}^* V_{\rm cs} + V_{\rm ub}^* V_{\rm us})$, we can write the amplitude in terms of two reduced matrix elements such that the corresponding decays of the B^0 and $\bar{B}^0$ will have the form

$$\begin{aligned} A(\pi^- K^+) &= V_{\rm ub}^* V_{\rm us}\, |U|\, e^{i\delta_U} + V_{\rm cb}^* V_{\rm cs}\, |C|\, e^{i\delta_C}\,, \\ \bar{A}(\pi^+ K^-) &= V_{\rm ub} V_{\rm us}^*\, |U|\, e^{i\delta_U} + V_{\rm cb} V_{\rm cs}^*\, |C|\, e^{i\delta_C}\,, \end{aligned} \tag{6.14}$$

where the reduced matrix element C comes from the penguin diagram alone and U comes from a mixture of tree and penguin effects. The decay rates for these two processes will then be different by a factor

$$|A(\pi^- K^+)|^2 - |\bar{A}(\pi^+ K^-)|^2 = -4|U||C| \sin(\delta_U - \delta_C)\lambda^6 A^2 \eta, \tag{6.15}$$

where we have used $\text{Im}\, V_{\rm ub}^* V_{\rm us} V_{\rm cb} V_{\rm cs}^* = \lambda^6 A^2 \eta$ in the Wolfenstein parameterization. This effect has required two paths to the given final state, with differing strong phases and differing weak phases. Because the hadronic matrix elements are difficult to calculate reliably, this rate difference cannot by itself be a precision test of the Standard Model.

However, there is a way to make an approximate test of the Standard Model using corresponding decays of the B_s meson. The key point [He 99, Gr 00] is that the tree process $b \to u\bar{u}d$ and the penguin amplitude for $b \to d\bar{q}q$ proceed identically to the corresponding processes used above for $b \to u\bar{u}s$ and $b \to s\bar{q}q$ aside from CKM factors. In the U-spin subgroup of $SU(3)$ the d and s quarks form a doublet, and all other quarks are singlets. The two sets of interactions then form two components of a U-spin doublet, and their matrix elements are related. B_d and B_s are also related by U-spin, so that the matrix elements for $B_d \to \pi^- K^+$ and $B_s \to K^- \pi^+$ are U-spin reflections of each other. The corresponding rates for B_s decay are given in the U-spin limit by

$$A_s(K^-\pi^+) = V_{\rm ub}^* V_{\rm ud}\,|U|\,e^{i\delta_U} + V_{\rm cb}^* V_{\rm cd}\,|C|\,e^{i\delta_C}\,,$$
$$\bar{A}_s(K^+\pi^-) = V_{\rm ub} V_{\rm ud}^*\,|U|\,e^{i\delta_U} + V_{\rm cb} V_{\rm cd}^*\,|C|\,e^{i\delta_C}. \qquad (6.16)$$

The weak CKM elements are different, but the hadronic matrix elements are the same. However, the Standard Model has only a single *CP*-violating phase, so the the imaginary parts of the products of CKM elements are always related. In this case, they are identical up to a sign Im $V_{\rm ub}^* V_{\rm ud} V_{\rm cb} V_{\rm cd}^* = -\lambda^6 A^2 \eta$, such that the decay rate differences are the same

$$|A(\pi^- K^+)|^2 - |\bar{A}(\pi^+ K^-)|^2 = -(|A_s(K^-\pi^+)|^2 - |\bar{A}_s(K^+\pi^-)|^2). \qquad (6.17)$$

However, asymmetries are defined by dividing by the the sum of the decay rates, and the overall decay rates are different in these two cases. Correcting for the overall rates yields a sum-rule [Li 05]

$$Q = A_{CP}(B_s \to K^-\pi^+) + A_{CP}(B_d \to \pi^- K^+)\frac{\mathrm{Br}(B_d \to \pi^- K^+)\tau_s}{\mathrm{Br}(B_s \to K^-\pi^+)\tau_d} = 0, \qquad (6.18)$$

where Br is the *CP*-averaged branching ratio. Despite the individual rates and asymmetries being different, the sum-rule appears valid within error bars [Aa *et al.* (LHCb collab.) 13*c*]

$$A_{CP}(B_s \to K^-\pi^+) = 0.27 \pm 0.04 \pm 0.01,$$
$$A_{CP}(B_d \to \pi^- K^+) = -0.080 \pm 0.007 \pm 0.003,$$
$$Q = -0.02 \pm 0.05 \pm 0.04. \qquad (6.19)$$

While the use of U-spin symmetry is only approximately accurate, this sum-rule nevertheless is a strong test of the overall pattern of direct *CP* violation within the Standard Model, including loop diagrams.

Semileptonic asymmetries

For a final example involving mixing, let us consider *CP* violation in semileptonic decays. In much of our previous analysis, we have neglected the quantity Γ_{12}. However, for semileptonic decays, the whole effect vanishes if we neglect Γ_{12}, so we must include it. For this case, only the transitions $B^0 \to \ell^+ \nu_\ell X$, $\bar{B}^0 \to \ell^- \bar{\nu}_\ell X$ ($\ell = e, \mu, \tau$) can occur. The 'wrong sign' transitions in the time developments, $B^0(t) \to \ell^- \bar{\nu}_\ell X$, $\bar{B}^0(t) \to \ell^+ \nu_\ell X$, are then uniquely due to mixing. The appropriate formulas can be obtained from our general result Eqs. (6.5a), (6.5b) by the substitutions

https://doi.org/10.1017/9781009291033.015 Published online by Cambridge University Press

$$A(e^-) \to 0, \quad A(e^-)\bar{\rho}(e^-) \to \bar{A}(e^-)\ ,$$
$$\bar{A}(e^+) \to 0, \quad \bar{A}(e^+)\rho(e^+) \to A(e^+) = \bar{A}(e^-). \tag{6.20}$$

The integrated rate is

$$A_{\rm SL} = \frac{\int_0^\infty dt\,\left[\Gamma_{B^0(t)\to\ell^-\bar{\nu}_\ell X} - \Gamma_{\bar{B}^0(t)\to\ell^+\nu_\ell X}\right]}{\int_0^\infty dt\,\left[\Gamma_{B^0(t)\to\ell^-\bar{\nu}_\ell X} + \Gamma_{\bar{B}^0(t)\to\ell^+\nu_\ell X}\right]} = \frac{\left|\frac{q}{p}\right|^2 - \left|\frac{p}{q}\right|^2}{\left|\frac{q}{p}\right|^2 + \left|\frac{p}{q}\right|^2}. \tag{6.21}$$

This sort of *CP* violation is thus solely sensitive to mixing in the mass matrix, as was the semileptonic K_L^0 asymmetry. Unfortunately, in the Standard Model it is small for reasons connected to the CKM elements. Expanding in powers of Γ_{12} and defining $\varphi_\Gamma \equiv \arg\left(\Gamma_{12}/M_{12}\right)$, one has

$$A_{\rm SL} \simeq -{\rm Im}\frac{\Gamma_{12}}{M_{12}} = -\left|\frac{\Delta\Gamma}{\Delta m}\right| \sin\varphi_\Gamma. \tag{6.22}$$

We have seen that $\Delta\Gamma/\Delta m$ is suppressed by factors of m_b^2/m_t^2 since the top quark cannot contribute to the real intermediate states required for $\Delta\Gamma$. For B_s, there is a further suppression in the Standard Model because the dominant contributions to Γ_{12} ($c\bar{c}$ intermediate states coming with CKM elements $(V_{\rm cb}^* V_{\rm cs})^2$) and M_{12} ($t\bar{t}$ intermediate states with $(V_{\rm tb}^* V_{\rm ts})^2$) have almost the same phase because $V_{\rm tb}^* V_{\rm ts} = -V_{\rm cb}^* V_{\rm cs}[1 + \mathcal{O}(\lambda^2)]$. Thus, φ_{Γ_s} is also suppressed to a fraction of a percent. These features are seen in the theoretical predictions [LeN 11]

$$A_d^{\rm SL}[{\rm Thy}] = (4.1 \pm 0.6) \times 10^{-4}, \qquad A_s^{\rm SL}[{\rm Thy}] = (1.9 \pm 0.3) \times 10^{-5}. \tag{6.23}$$

The present experimental results [RPP 12, Ve (LHCb collab.) 13],

$$A_d^{\rm SL}[{\rm Expt}] = 0.0007 \pm 0.0027, \qquad A_s^{\rm SL}[{\rm Expt}] = -0.0024 \pm 0.0054 \pm 0.0033, \tag{6.24}$$

are not yet precise enough to confirm the Standard Model predictions.

CP-odd signals not induced by mixing

Situations where *CP* violation occurs *without* the presence of mixing can occur in $B^\pm$ decays through the interference of different decay mechanisms. The requirements are the same as we saw previously in a different context, i.e., there must be two different paths to the same final state, these paths must have different strong-interaction final-state phases, and the two paths must also have different weak phases. Consider, for example, the decays $B^+ \to D^0 K^+$ and $B^+ \to \bar{D}^0 K^+$. While initially one might think that these two reactions are distinct, if the D^0 and $\bar{D}^0$ decay to a common final state, such as $K_S^0\pi^+\pi^-$, the overall amplitudes to that

https://doi.org/10.1017/9781009291033.015 Published online by Cambridge University Press

final state will in fact interfere. The decay with a D^0 in the final state involves the $\bar{b} \to \bar{u}c\bar{s}$ reaction, with CKM elements $V_{\rm ub}^* V_{\rm cs}$, while the $\bar{D}^0$ reaction proceeds through $\bar{b} \to \bar{c}u\bar{s}$ and $V_{\rm cb}^* V_{\rm us}$. The relative phase between these amplitudes is the angle γ.

Interestingly, despite the need for final-state phases in this reaction, the *CP* violation can be extracted without hadronic uncertainties [GrW 91, GiGSZ 03]. The key to this is that the subreaction $D^0 \to K_S^0 \pi^+\pi^-$ can be separately measured in tagged D reactions as a function of the kinematic variables, and then can be treated as a known quantity. In addition the D^0 and $\bar{D}^0$ decay amplitudes are related to each other[12] at mirror kinematic values. In particular, if the decay $D^0 \to K_S^0 \pi^+\pi^-$ is given the name $A(m_+^2, m_-^2)$ with $m_\pm^2 = (p_K + p_\pm)^2$ then the corresponding $\bar{D}^0$ amplitude is $\bar{A}(m_+^2, m_-^2) = A(m_-^2, m_+^2)$. The amplitudes, including the possibility of final-state interaction phases, have the form

$$|A_{B^+ \to (K_S\pi^+\pi^-)K^+}|^2 = |A_0|^2 |A(m_+^2, m_-^2) + r\bar{A}(m_+^2, m_-^2)e^{\delta+\gamma}|^2,$$
$$|A_{B^- \to (K_S\pi^+\pi^-)K^-}|^2 = |A_0|^2 |\bar{A}(m_+^2, m_-^2) + rA(m_+^2, m_-^2)e^{\delta-\gamma}|^2, \qquad (6.25)$$

where an overall amplitude for $A_0 \equiv A_{B^+ \to D^0 K^+}$ has been factored out and where r is the ratio of the magnitudes of the amplitudes $r = |A_{B^+ \to \bar{D}^0 K^+}|/|A_{B^+ \to D^0 K^+}|$. Here, the possible strong-phase difference δ has been made explicit. Knowledge of the D decay amplitudes plus the observation of both $B^\pm$ decays then lets one separate the strong phase from the weak phase and also divide out the underlying weak matrix elements. This has become a favored way to measure the angle γ with the present result [Aa *et al.* (LHCb collab.) 12],

$$\gamma = (71.1^{+16.6}_{-15.7})^o, \qquad (6.26)$$

when all related channels are included.

To summarize, we have discussed thus far a variety of tests for *CP*-violating signals in the system of B mesons. The partial rate differences can be quite large. At first, this seems to go against the general dictum that all *CP* violations in the Standard Model must be proportional to a single, numerically small product of CKM angles. However, B decays satisfy this stricture in the sense that the mixing and decay of B mesons are in themselves proportional to small CKM angles. Overall, the product of mixing, decay, and *CP* violation does turn out to be proportional to all of these CKM angles. However, in forming the asymmetry by dividing out the rates themselves, one is canceling the small CKM angles, thus leaving a rather large effect. This argument also explains why there is little *CP* violation in D decays in the Standard Model. The *CP* observables must be small due to the usual product of CKM angles. However, the overall decay rate itself has no small

[12] Here we neglect *CP* violation in the D-meson system, which is a good approximation for CKM-favored decays.

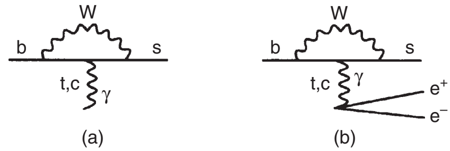

Fig. XIV–6 Some one-loop diagrams for rare B decays.

angles, so that the signal remains small. B-meson decays have proven to be optimal for the exploration of the rich CP-violating structure of the Standard Model.

XIV–7 Rare decays of *B* mesons

The number of B-decay modes is so large that *any* single mode will be 'rare' in the sense of having a small branching ratio. Nonetheless, considerable attention has been given to modes that proceed *only* at one loop, as in Fig. XIV–6, and these are the ones that are normally labeled as rare decays. The expectation is that, by measuring the transition rates of such processes, one can test the Standard Model at loop level, and hopefully observe deviations due to New Physics. Moreover, since prediction of rare decays involves many of the techniques we have developed for calculating weak transitions, these decays can provide a nontrivial test of our ability to apply the Standard Model.

The quark transition $b \to s\gamma$

The process $b \to s\gamma$ is described by the magnetic-dipole transition

$$\mathcal{M}_{b\to s\gamma} = \frac{G_F}{\sqrt{2}}\frac{e}{8\pi^2}F_2 V_{\rm cb}V_{\rm cs}^*\epsilon^*(\mathbf{q})^\mu q^\nu \\ \times \bar{u}(\mathbf{p}_s)\sigma_{\mu\nu}\left[m_b\left(1-\gamma_5\right)+m_s\left(1+\gamma_5\right)\right]u(\mathbf{p}_b), \qquad (7.1)$$

where the quark mass factors occur in the combination shown because the $\sigma_{\mu\nu}$ Dirac matrix connects left-handed fields to right-handed fields, and a factor of mass must appear whenever a chirality change $L \to R$ occurs.

The quantity F_2, which represents the quark-level loop amplitude with numerical factors containing G_F and e extracted, is given by

$$F_2 \simeq \bar{F}_2\left(x_t\right) - \bar{F}_2\left(x_c\right) \simeq \bar{F}_2\left(x_t\right), \qquad (7.2)$$

with $x_i = m_i^2/M_W^2$ and

$$\bar{F}_2(x) = \frac{x}{(x-1)^3}\left[\frac{2x^2}{3}+\frac{5x}{12}-\frac{7}{13}-\left(\frac{3x^2}{2}-x\right)\ln x\right]. \qquad (7.3)$$

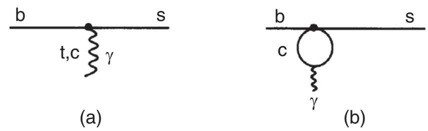

Fig. XIV–7 Standard Model diagrams for $b \to s\gamma$.

The flavor content of F_2 and the overall factor of $V_{\rm cb}V^*_{\rm cs}$ in Eq. (7.1) can be easily understood. The overall loop amplitude, which involves a sum over the intermediate quark flavors t, c, u, must vanish in the limit of equal quark mass from a GIM cancelation since it involves a neutral flavor-changing process. In reality, however, the contribution from the very light u quark is negligible, and the top-quark contribution to F_2 clearly dominates. The CKM unitarity relation $V_{\rm tb}V^*_{\rm ts} = -V_{\rm cb}V^*_{\rm cs} - V_{\rm ub}V^*_{\rm us}$ can be used to substitute for $V_{\rm tb}V^*_{\rm ts}$ upon neglecting the small factor $V_{\rm ub}V^*_{\rm us}$. The $b \to s\gamma$ decay rate, relative to the $b \to ce\bar{\nu}_e$ semileptonic rate can be expressed in the simple form

$$\frac{\Gamma_{b\to s\gamma}}{\Gamma_{b\to ce\bar{\nu}_e}} = \frac{3\alpha|F_2|^2}{f(m_c/m_b)}, \tag{7.4}$$

where $f(x)$ is the phase-space factor given in Eq. (2.1), and factors of m_s^2/m_b^2 arising from phase space and from the amplitude of Eq. (7.1) have been dropped.

Short-distance *QCD* corrections can be used to improve this free-quark calculation. These produce a surprisingly large modification to the analysis of $b \to s\gamma$, and the reason is instructive. The t quark is so heavy that, at all scales relevant to the weak decay, its effect may be treated as a point $bs\gamma$ vertex, with renormalizations as in Fig. XIV–7(a). However, the c quark is light on all scales from M_W to m_b so that in its renormalization one must also include the diagrams of Fig. XIV–7(b), where the dot represents the $b \to c\bar{c}s$ weak hamiltonian. That is, there is mixing between the $b \to s\gamma$ vertex and the $b \to c\bar{c}s$ transition. The theoretical prediction is [Mi *et al*. 07],

$$\mathcal{B}_{b\to s\gamma}[\text{Thy}] = (3.15 \pm 0.23) \times 10^{-4}, \tag{7.5}$$

for photon energies above 1.6 GeV. The corresponding measurement (highly nontrivial) is [Am *et al.* (Heavy Flavor Averaging Group collab.) 12]

$$\mathcal{B}_{b\to X_s\gamma}[\text{Expt}] = (3.55 \pm 0.24 \pm 0.09) \times 10^{-4}, \tag{7.6}$$

where the last error bar is due to uncertainties in the treatment of the photon energy distribution.

At the hadronic level, the quark transition $b \to s\gamma$ is observed in channels such as $B \to K\pi\gamma$, $K\pi\pi\gamma$, etc. The simplest final state occurs when the $K\pi$ system

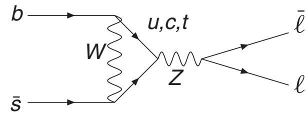

Fig. XIV–8 The penguin diagram for $B_s \to \ell^+\ell^-$.

forms a resonant $J^P = 1^-$ state, $K^*(890)$.[13] As the inclusive rate appears to be in agreement with the Standard Model, this effort is a test of the calculation of exclusive transitions. Within the same class of decays is the transition $B \to K^*\ell^+\ell^-$. Theoretical interest in this transition comes from the hope that New Physics not present in $B \to X_s\gamma$ could show up here [DeHMV 13]. The amplitude includes Z^0 as well as photon exchange, and the loops could be sensitive to new interactions. Experimentally, the decay is rich and challenging because a full angular distribution can be probed, with the possibility of sensitivity to different physics in different kinematic regions.

The decay $B_s \to \ell^+\ell^-$

The leptonic transition $B_s \to \ell^+\ell^-$ is also particularly promising as a sensitive test of the Standard Model. The rate is suppressed even more by a factor of m_ℓ^2 due to a helicity argument which relies on the current–current structure of the theory, and this allows New Physics to be present.

The decay proceeds through the Z^0 penguin diagram of Fig. XIV–8 with the dominant contribution from the top quark due to its large mass. The photon penguin does not contribute because the photon as a vector has $C = -1$, while the lepton–antilepton pair with zero angular momentum has $C = +1$. The transition then occurs through the axial-vector Z^0 current, with an effective hamiltonian,

$$H = \frac{G_F\alpha}{2\sqrt{2}\pi\ \sin^2\theta_W} V_{\rm tb}^* V_{\rm ts} \mathcal{C}_A \bar{b}\gamma^\mu\gamma_5 s\ \bar{\ell}\gamma_\mu\gamma_5\ell, \tag{7.7}$$

where, as usual, $\mathcal{C}_A$ is a coefficient which includes the *QCD* short-distance corrections. When computing the decay amplitude, we encounter the matrix element

$$\langle 0|\bar{b}\gamma^\mu\gamma_5 s|B_s(q)\rangle = iF_{B_s}q^\mu, \tag{7.8}$$

and the q^μ contracted with the lepton current produces a factor of m_ℓ in direct analogy to the pion decay discussed in Chap. VII. Note that scalar or pseudoscalar interactions would not have such suppression and so these New Physics possibilities

[13] The $B \to K\gamma$ transition is forbidden because it is a spin-zero to spin-zero transition.

https://doi.org/10.1017/9781009291033.015 Published online by Cambridge University Press

could potentially have a large enhancement over the Standard Model prediction. The theoretical prediction [BuGGI 12, DeFKKMPT 12]

$$\mathcal{B}^{(\text{theo})}_{B_s\to\mu^+\mu^-} = (3.54 \pm 0.30) \times 10^{-9} \tag{7.9}$$

is quite robust, with the major uncertainty being the lattice calculation of F_{B_s}. This mode has recently been measured [Aa *et al.* (LHCb collab.) 13*b*] with the result,

$$\mathcal{B}^{(\text{expt})}_{B_s\to\mu^+\mu^-} = \left(3.2^{+1.5}_{-1.2}\right) \times 10^{-9}. \tag{7.10}$$

An even more recent result, although preliminary, shows that combined LHCb and CMS data agree with the Standard Model prediction by more than 5σ. This clearly indicates that there is no large effect from New Physics.

Problems

(1) **Patterns of *CP* violation**
All signals of *CP* violation involve the interference of two or more amplitudes. Identify the origin of the interference in partial rate asymmetries for the decays (a) $B_s \to \varphi\varphi$, (b) $B_s \to \rho^\pm\pi^\mp$, (c) $B_d \to \bar{K}^{*0}\varphi$, (d) $B^\pm \to \rho^\pm\pi^0$, (e) $B^\pm \to K^\pm\pi^0$.

(2) **Amplitude relations in the heavy-quark limit**
In the heavy-quark limit, a static b quark in a B meson can be described in terms of just the two upper components of its four-component Dirac field. This can simplify various matrix elements or be used to relate them. Use this feature to show that the $\bar{B} \to K^*\gamma$ matrix element of the $\sigma^{\mu\nu}$ operator,

$$\langle K^*(\epsilon, \mathbf{k})|\bar{s}\sigma^{\mu\nu}b|\bar{B}(\mathbf{p})\rangle = \epsilon^{\mu\nu\alpha\beta}\left[A\,\epsilon^\dagger_\alpha p_\beta + B\,\epsilon^\dagger_\alpha k_\beta + \epsilon^\dagger\cdot p\;C\;p_\alpha k_\beta\right],$$

can be related to the vector and axial-vector form factors of $\bar{B} \to \rho\ell\bar{\nu}_\ell$,

$$\langle \rho^+(\epsilon, \mathbf{k})|\bar{u}\gamma^\mu b|\bar{B}^0(\mathbf{p})\rangle = i\,D\,\epsilon^{\mu\nu\alpha\beta}p_\nu\epsilon^\dagger_\alpha k_\beta,$$
$$\langle \rho^+(\epsilon, \mathbf{k})|\bar{u}\gamma^\mu\gamma_5 b|\bar{B}^0(\mathbf{p})\rangle = E\,\epsilon^{\dagger\mu} + \epsilon^\dagger\cdot p\,[Fp^\mu + Gk^\mu],$$

through

$$A = -(E - k_0 m_B D)/m_B, \quad B = -m_B D, \quad C = (D + G)/m_B,$$

under the assumptions of a static b quark and of $SU(3)$ symmetry. In this relation, all form factors must be evaluated at the same momentum transfer, $q^2 = (p - k)^2$.

https://doi.org/10.1017/9781009291033.015 Published online by Cambridge University Press